Title: The zebrafish orthologue of familial Alzheimer's disease gene *PRESENILIN 2* is required for normal adult melanotic skin pigmentation.

Authors: Haowei Jiang[1,*], Morgan Newman[1], Michael Lardelli[1]

Affiliations: [1]University of Adelaide, School of Biological Sciences, Alzheimer's Disease Genetics Laboratory, North Terrace, Adelaide, SA 5005, AUSTRALIA

***Corresponding Author:** Haowei Jiang, University of Adelaide, School of Biological Sciences, Alzheimer's Disease Genetics Laboratory, North Terrace, Adelaide, SA 5005, AUSTRALIA. Email: haowei.jiang@adelaide.edu.au

Key words: CRISPR/Cas9, familial Alzheimer's disease, PRESENILIN 2, pigmentation, zebrafish

Abbreviations: AD, Alzheimer's Disease; CRISPR, clustered regularly interspaced short palindromic repeats; DSB, double-strand break; HDR, homology-directed repair ; NHEJ, nonhomologous end joining; NMD, nonsense-mediated decay; PSEN, PRESENILIN; PTC, premature translation-termination codon; TMD, transmembrane domain;

Financial Disclosure Statement: This research was supported by grants from the National Health and Medical Research Council of Australia, GNT1061006 and GNT1126422, and by funds from the School of Biological Sciences of the University of Adelaide. HJ is supported by an Adelaide Scholarship International from the University of Adelaide.

Conflict of Interest Statement: The authors declare no conflict of interest.

Abstract

Alzheimer's disease is the most common form of age-related dementia. At least 15 mutations in the human gene *PRESENILIN 2* (*PSEN2*) have been found to cause familial Alzheimer's disease (fAD). Zebrafish possess an orthologous gene, *psen2*, and present opportunities for investigation of *PRESENILIN* function related to Alzheimer's disease. The most prevalent and best characterized fAD mutation in *PSEN2* is *N141I*. The equivalent codon in zebrafish *psen2* is N140. We used genome editing technology in zebrafish to target generation of mutations to the N140 codon. We isolated two mutations: $psen2^{N140fs}$, (hereafter "*N140fs*"), causing truncation of the coding sequence, and $psen2^{T141\_L142delinsMISLISV}$, (hereafter "*T141_L142delinsMISLISV*"), that deletes the two codons immediately downstream of N140 and replaces them with seven codons coding for amino acid residues MISLISV. Thus, like almost every fAD mutation in the *PRESENILIN* genes, this latter mutation does not truncate the gene's open reading frame. Both mutations are homozygous viable although *N140fs* transcripts are subject to nonsense-mediated decay and lack any possibility of coding for an active γ-secretase enzyme. *N140fs* homozygous larvae initially show grossly normal melanotic skin pigmentation but subsequently lose this as they grow while retaining pigmentation in the retinal pigmented epithelium. *T141_L142delinsMISLISV* homozygotes retain faint skin melanotic pigmentation as adults, most likely indicating that the protein encoded by this allele retains weak γ-secretase activity. Null mutations in the human

PRESENILIN genes do not cause Alzheimer's disease so these two mutations may be useful for future investigation of the differential effects of null and fAD-like *PRESENILIN* mutations on brain aging.

Introduction

Alzheimer's disease (AD) is a progressive neurodegenerative disorder, and is the most common form of age-related dementia, accounting for 50-75% of dementia cases worldwide (1). Most AD occurs after the age of 65 years (late onset) and is sporadic. Early onset AD is far less common and approximately 13% of early onset cases are familial AD (fAD) (2). Autosomal dominant inheritance of mutations in the *AMYLOID BETA A4 PRECURSOR PROTEIN* gene (*APP*) (3), *PRESENILIN 1* and *2* genes (*PSEN1*, *PSEN2*) (4), and *SORTILIN-RELATED RECEPTOR* gene (*SORL1*) (5, 6) are considered to be the major cause of fAD. Of the two *PRESENILIN* genes, *PSEN2* is a less common locus for fAD mutations than *PSEN1*. Only around 15 fAD mutations have been reported in *PSEN2* to date, compared to over two hundred mutations reported in *PSEN1* (4). All but one of the many different fAD mutations in the *PSEN* genes do not cause truncation of coding sequences, a phenomenon we have previously described as the "fAD mutation reading frame preservation rule" (7).

PSEN proteins become endoproteolytically cleaved during activation of γ-secretase activity to form N- and C-terminal fragments (NTF and CTF resprectively) (8). The

NTFs and CTFs of PSEN2 predominantly localise to the endoplasmic reticulum (ER) (9) and to late endosomes / lysosomes (10). The first two transmembrane domains (TMDs) of PSEN2 are thought to be necessary for ER localisation (11) while a conserved sequence near the N-terminal is bound by Adaptor Complex AP-1 to direct PSEN2 protein to late endosomes / lysosomes (10). The localisation of PSEN2, rather than PSEN1, to late endosomes / lysosomes implies a particular importance for PSEN2 in the biogenesis of melanosomes (10, 12), an organelle type related to lysosomes (13) that is specialised for formation of the dark pigment melanin (14).

The first fAD mutation reported in *PSEN2* was *N141I*, caused by an A-to-T transition at the second position of codon 141 (15). The *N141I* mutation alters the N-terminal flank of the second TMD (TMD2) of PSEN2 by substituting a hydrophobic isoleucine residue for the hydrophilic asparagine residue immediately downstream of the first residue of TMD2. This position is thought to be important for accurate positioning of the transmembrane α-helix structure (16). A PolyPhen-2 (17) analysis of the *N141I* mutation indicates probable damage to protein structure with a score of 0.934 (sensitivity: 0.80; specificity: 0.94). The mean age of Alzheimer's disease onset for carriers of *N141I* is 53.7 years old, but with a very wide range of 39 to 75 years (4). Thus, *N141I* has an age of onset overlapping those of *PSEN1* fAD families (mean age of onset of 45.5 years) and sporadic AD (mean age of onset of 71.5) (4). The *N141I* mutation is thought to increase the ratio of Aβ42 to Aβ40 via abnormal γ-secretase activity (18). A more recent transgenic mouse model of AD suggested that both Aβ42

and Aβ40 production are enhanced by *N141I*, and this can signficantly accelerate Aβ-dependent dysfunction in spatial learning and memory (19).

Mammalian PRESENILINs have also been found necessary for tyrosinase trafficking and melanin formation by a γ-secretase-dependent mechanism (20). TYROSINASE is a key enzyme in melanin synthesis (21). The two TYROSINASE-related proteins, TYROSINASE-related protein 1 (Tyrp1) and DOPACHROME TAUTOMERASE (DCT) (also known as TYROSINASE-related protein 2 (Tyrp2)) (22), are implicated in the activity of the intramembrane protease, γ-secretase (20, 23). A partial loss-of-function in melanotic pigment formation has been observed in a mouse model of the *PSEN1* fAD mutation *M146V* (20).

In mammals, the protein SILVER, MOUSE, HOMOLOG OF (SILV, also known as PREMELANOSOMAL PROTEIN, PMEL) (24) is another type 1 membrane protein that can be cleaved by proteases including γ-secretase (25) to form a natural functional amyloid that facilitates melanin formation (12). SILV is expressed in pigment cells of the eye and skin, which synthesise melanin pigments within melanosomes (26). After a juxtamembrane cleavage, the C-terminal fragment of SILV is then processed by the γ-secretase complex to release an intracellular domain fragment (25) into endosomal precursors to form amyloid fibrils. These ultimately become melanosomes (27, 28).

Zebrafish are a versatile system in which to investigate, at the molecular level, the effects on the brain and other tissues of fAD mutations (29). The ability to generate large families of siblings and then raise these in a near identical environment (the same tank or the same recirculated-water system) can reduce genetic and environmental variability to allow more sensitive detection of mutation-dependent changes. The organisation of the genome and the genetic pathways controlling signal transduction and development of zebrafish and humans are highly conserved (30). Despite ~420 million years of divergent evolution of the human and zebrafish lineages (31), most human genes have clearly identifiable orthologues in zebrafish. Thus, the zebrafish genes *psen1* (32) and *psen2* (33) are orthologues of human *PSEN1* and *PSEN2*, respectively. The Presenilin protein sequences of zebrafish show considerable identity with those of humans. The zebrafish Psen1 protein shows 73.9% amino acid residue (aa) identity with human PSEN1 (32), while zebrafish Psen2 shows 74% identity with human PSEN2 (33).

In this paper, we describe an attempt to generate a zebrafish model of the *N141I* fAD mutation of human *PSEN2* by introducing an equivalent mutation into the zebrafish *psen2* gene. While homology-directed repair (HDR) after CRISPR Cas9 cleavage at the relevant site in zebrafish *psen2* was not successful, we did find products of non-homologous end joining (NHEJ) that will prove useful in future analyses. We identified both a frameshift mutation and a reading frame-preserving indel mutation close to the N141-equivalent codon of zebrafish *psen2* (N140). Surprisingly, we

discovered that the γ-secretase activity of Psen2 (unlike that of Psen1) appears essential for melanotic pigment formation in the skin of zebrafish adults but not in their retinal pigmented epithelium.

Materials and Methods

Animal ethics

All experiments using zebrafish were conducted under the auspices of the Animal Ethics Committee of the University of Adelaide. Permits S-2014-108 and S-2017-073.

CRISPR guide RNA (sgRNA) design and synthesis

The target sequence of the sgRNA used to generate double-stranded breaks near the N140 codon in zebrafish *psen2* is 5'-GAATTCGGTGCTCAACACTC *TGG*-3'. The template for sgRNA transcription was synthesised by PCR (34). The forward primer for this template synthesis PCR contains a T7 polymerase binding site (the underlined region), the target sequence (bold) and a region complementary to a common reverse primer (italicised):

5'-GAAATTAATACGACTCACTATAGG**GAATTCGGTGCTCAACACTC***GTTTT AGAGCTAGAAATAGC*-3'. The sequence of the reverse primer is 5'-AAAAGCACCGACTCGGTGCCACTTTTTCAAGTTGATAACGGACTAGCCTTA

TTTTAACTTGCTATTTCTAGCTCTAAAAC-3'. This synthesis PCR used Phusion® High-Fidelity DNA Polymerase (NEB, Ipswich, Massachusetts, USA, M0530S) and cycle conditions of 98°C for 30 s and then 35 cycles of [98°C, 10 s; 60°C, 30 s; 72°C, 15 s] then 72°C, 10 min. The template was then gel-purified using the Wizard® SV Gel and PCR Clean-Up System (Promega, Madison, Wisconsin, USA, A9281). The target sgRNA was synthesized from this template using the HiScribe™ T7 Quick High Yield RNA Synthesis Kit (NEB, Ipswich, Massachusetts, USA, E2050S).

Design of single-stranded oligonucleotide templates for homology-directed repair (HDR)

To attempt to introduce the *N140I* mutation into zebrafish *psen2* (equivalent to human *PSEN2 N141I*), a single stranded oligonucleotide template ("N140I oligo") containing the N>I mutation (A>T, bold italics and underlined) followed by two silent (synonymous codon) mutations (T>C and G>C, italicised and underlined) was designed:

5'-ACTCAGTGGGCCAGCGTCTGCTGAATTCGGTGCTC***A<u>T</u>C***AC<u>C</u>CT<u>C</u>GTCATG ATCAGTGTGATTGTCTTCATGACC-3'.

We also attempted (unsuccessfully) to introduce the *V147I* mutation into zebrafish *psen2*, (equivalent to *V148I* in human *PSEN2*) using a single-stranded oligonucleotide template ("V147I oligo"), containing the V>I mutation (G>A and G>C, bold italics

and underlind) followed by two silent (synonymous codon) mutations (T>A and C>G, italicised and underlined): 5'-CTGAATTCGGTGCTCAACACTCTGGTCATGATCAGT***A*****T*****C***AT*A*GT*G*TTCATGACCATCATCCTGGTGCTGCTCTAC-3'. The attempted mutation of the *V147* site in *psen2* is only described and discussed in Supplemental Information.

The single-stranded oligonucleotide templates were co-injected with their corresponding CRISPR/Cas9 systems, so that any induced double-stranded DNA breaks (DSBs) might be repaired through the HDR pathway (35) to insert desired mutations into the zebrafish genome.

Injection of zebrafish embryos

Tübingen (TU) strain wild type embryos were collected from mass spawning. The target sgRNA (70 ng/μL final concentration) was mixed with "N140I oligo" (30 ng/μL for final concentration) and Cas9 nuclease (1μg/μL for final concentration) (Invitrogen, Carlsbad, California, USA, B25640), and then incubated at 37°C for 15 min to maximize formation of active CRISPR Cas9 complexes. 5-10 nL of the mixture was then injected into zebrafish embryos at the one-cell stage. The injected embryos were subsequently raised for mutation screening.

Mutation detection in CRISPR Cas9-injected G0 fish

From each batch of injected embryos, 10 embryos were selected at random at ~24 hpf and pooled for genomic DNA extraction. The genomic DNA of these embryos was extracted using sodium hydroxide (36). The 10 embryos were placed in 100 μL of 50 mM NaOH and then heated to 95°C for 15 min. They were then cooled to 4°C followed by addition of 1/10th volume of 1 M Tris-HCl, pH 8.0 to neutralize the basic solution (36).

Mutation-specific primers were designed to detect mutation-carrying fish by PCR. For the "N140I oligo"-injected embryos, a mutation-specific forward primer was designed: 5'-TCGGTGCTC***A*****T*****C***AC*C*CT*C*-3'. A wild type-specific forward primer (5'-TCGGTGCTC*AACACTCTG*-3') and a common reverse primer (5'-ACCAAGGACCACTGATTCAGC-3') were also designed. The PCR conditions for both these reactions are: 95°C, 2 min and then 31 cycles of [95°C, 30 s; 58°C, 30 s; 72°C 30 s], then 72°C, 5 min. The lengths of the expected PCR products of these reactions are all ~300 nucleotides.

For the "V147I oligo"-injected embryos, a mutation-specific forward primer was designed: 5'-TCTGGTCATGATCAGT***A*****T*****C***AT*A*GT*G*-3'. A wild type-specific forward primer (5'-TCTGGTCATGATCAGT*GTGATTGTC*-3') and a common reverse primer (5'-TCACCAAGGACCACTGATTCAGC-3') were also designed. The PCR conditions for all these three reactions are: 95°C, 2 min, and then 31 cycles of [95°C,

30 s; 58°C, 30 s; 72°C, 30 s], then 72°C 5 min. The lengths of the PCR products of these reactions are ~280 nucleotides.

The F1 progeny of the mosaic, mutation-carrying G0 fish were also screened with these mutation-specific PCR reactions.

Mutation detection in F1 fish using the T7 endonuclease I assay

Since the DSBs induced by the CRISPR/Cas9 system may also be repaired through the NHEJ pathway (35, 37), random mutations may also be generated at the DSB sites. Thus, the F1 progeny of the mosaic, mutation-carrying G0 fish may be heterozygous for such random mutations.

To screen for these mutations, the genomic DNA of tail biopsies from F1 fish was extracted using sodium hydroxide as above, followed by analysis using the T7 endonuclease I assay (since T7 endonuclease I is able to recognize and cleave at the sites of mismatches in DNA heteroduplexes (38)).

A pair of amplification primers binding in the regions flanking the N140 target site was designed: 5'-AGCATCACCTTGATTCAAGG-3' and 5'-GGTTCCTGATGACACACTGA-3'. The PCR conditions for this amplification reaction are 95°C, 2 min and then 31 cycles of [95°C, 30 s; 58°C, 30 s; 72°C, 30 s],

then 72°C, 5 min and the amplified fragment is predicted to be 473 nucleotides in length. The PCR products were purified using the Wizard® SV Gel and PCR Clean-Up System (Promega, Wisconsin, USA, A9281). These purified PCR products were then denatured at 95°C for 5 min and then annealed by slow cooling of the samples at -2°C/sec from 95°C to 85°C and then -0.1°C/sec from 85°C to 25°C). Finally, the annealed PCR products were digested using T7 endonuclease I (NEB, Ipswich, Massachusetts, USA, M0302S) was added to. If reannealed fragments contained mismatches due to mutations, they would be cleaved by T7 endonuclease I into two fragments; ~109 nucleotides (upstream) and ~364 nucleotides (downstream). Those amplified and reannealed fragments showing positive signals (cleavage) in T7 endonuclease I assays were then sent to the Australian Genome Research Facility (AGRF, North Melbourne, VIC, Australia) for **S**anger sequencing to identify the mutations.

Mutation detection in F2 fish using PCR

Mutation-specific PCR primers were designed to detect the two mutations (*N140fs* and *T141_L142delinsMISLISV*) identified in F1 fish. For *N140fs*, a mutation-specific forward primer (5'-TGCTGAATTCGGTGCTCTG-3') was designed. For *T141_L142delinsMISLISV*, another mutation-specific forward primer (5'-TGAATTCGGTGCTCAACATG-3') was designed. A wild type-specific forward primer (5'-TGAATTCGGTGCTCAACACTC-3') was designed as a control. A

common reverse primer (5'-TCACCAAGGACCACTGATTCAGC-3') was used with these three different forward primers. The temperature cycling conditions for these PCRs are identical for the wild type and *N140fs* alleles: 95°C, 2 min, and then 31 cycles of [95°C, 30 s; 60°C, 30 s; 72°C, 30 s], then 72°C, 5 min. For detection of the *T141_L142delinsMISLISV* allele, the annealing temperature was altered to 61.5°C. The PCR products of these reactions are all predicted to be ~320 nucleotides in length.

Breeding of mutant fish

Since the mutation-carrying G0 fish were mosaic for mutations, these were outbred with wild type TU fish so that their progeny (F1 fish) would be completely heterozygous for any mutations.

The F1 fish carrying the *T141_L142delinsMISLISV* or *N140fs* alleles were outbred with wild type TU fish to generate additional individuals heterozygous for the mutations. (The families of progeny of such matings would consist of 50% heterozygous mutants and 50% wild type fish). When these F2 progeny were sexually mature, pairs of heterozygous individuals were in-crossed to generate F3 families containing homozygous mutant, heterozygous mutant and wild type siblings for further analysis.

295

296 **Imaging of skin pigmentation in zebrafish**

297

298 The pigmentation patterns of mutant zebrafish were imaged using a Leica
299 Microsystems, Type DFC450 C microscope, and the software Leica Application Suite,
300 Version 4.9.0 (Leica Microsystems, Wetzlar, Germany).

301

302 **Total RNA extraction from 6-month-old zebrafish brains**

303

304 When F2 fish families from outcrossed heterozygous mutant F1 fish were 6 months of
305 age, eight female fish of each genotype (i.e. eight wild type and eight heterozygous
306 mutant individuals) were selected for brain removal (after euthanized by submersion
307 in ice water) and total RNA extraction. From these fish, four of each genotype were
308 exposed to hypoxia according to the method we have previously established (39). The
309 dissolved oxygen content of the hypoxic water was ~1.00 mg/L (treated for ~2.5 h),
310 while the other four fish of each genotype were exposed to normoxia (i.e. the
311 dissolved oxygen content of the normoxic water was ~6.60 mg/L). Total RNA was
312 extracted from these brains using the *mir*Vana™ miRNA Isolation Kit (Ambion,
313 Inc, Foster City, California, USA, AM1560). cDNA was synthesised from the RNA
314 using the SuperScript™ III First-Strand Synthesis System (Invitrogen, Carlsbad,
315 California, USA, 18080051) and Random Primers (Promega, Madison, Wisconsin,
316 USA, C1181).

317

318 **Allele-specific expression analysis by digital quantitative PCR (dqPCR)**

319

320 PCR primer pairs detecting specific alleles were designed for dqPCR: a specific
321 forward primer for mutation *T141_L142delinsMISLISV*
322 (5'-TGAATTCGGTGCTCAACATG-3'), a specific forward primer for mutation
323 *N140fs* (5'-TGCTGAATTCGGTGCTCTG-3'), and a specific forward primer for
324 the wild type allele (5'-TGAATTCGGTGCTCAACACTC-3'). A common reverse
325 primer (5'-AAGAGCAGCATCAGCGAGG-3') was used with all these three forward
326 primers. Allele-specific dqPCR was performed using the QuantStudio™ 3D Digital
327 PCR System (Life Sciences, Waltham, MA, USA) with QuantStudio™ 3D Digital
328 PCR 20K Chip Kit v2 and Master Mix (Life Sciences, Waltham, MA, USA, A26317)
329 and SYBR™ Green I Nucleic Acid Gel Stain (Life Sciences, Waltham, MA, USA,
330 S7563). The dqPCR conditions for allele-specific expression detection are 96°C, 10
331 min, then 49 cycles of [62°C, 2 min; 98°C, 30 s], then 62°C 2 min. The expected
332 length of the PCR products is ~130 bp. 25ng of cDNA (based on quantification of
333 RNA concentration and the assumption of complete reverse transcription into cDNA)
334 of each sample was loaded into each chip. The chips were analysed using
335 QuantStudio™ 3D AnalysisSuite Cloud Software (Life Sciences, Waltham, MA,
336 USA).

337

338 ## Results

339

340 **fAD-like and coding sequence-truncating mutations in *psen2***

341

342 Our initial aim was to create mutations in zebrafish *psen2* equivalent to the fAD
343 mutations of human *PSEN2*, *N141I* and *V148I* (*N140I* and *V147I* in zebrafish
344 respectively). However, while CRISPR Cas9-targetting of these sites appeared
345 feasible, no incorporation of desired mutations via homology-directed repair was
346 found. Nevertheless, two mutations at the N140 site were ultimately identified. One of
347 these is an indel mutation removing two codons (T141 and L142) and replacing these
348 with seven novel codons (MISLISV). Consequently, this allele is designated
349 *T141_L142delinsMISLISV* and may be considered EOfAD-like in that it does not
350 truncate the coding sequence (CDS) (Fig 1). The second mutation is a deletion of 7
351 nucleotides causing a frameshift that does truncate the coding sequence, *N140fs*, due
352 to a premature termination codon (PTC) at the 142nd codon position.

353

354 **Fig 1. Predicted protein primary and secondary structures.**

355 (A) The protein coding sequence of zebrafish Psen2 is altered by the mutations.

356 (B) The predicted protein structures of zebrafish Psen2 are also changed by the two
357 identified mutations (and are shown relative to the wild type structure and a structure
358 incorporating a hypothetical *N140I* mutation. Purple bar: helix; yellow arrow: strand;
359 black line: coil; Conf: confidence of prediction; Pred: predicted secondary structure;
360 AA: target sequence.

Inbreeding of *T141_L142MISLISV* and *N140fs* mutant fish showed both mutations to be homozygous viable although both showed severe defects in skin pigmentation in post-larval stages (described later).

Changes of protein structure caused by the mutations

PRESENILINs have a complex structure with multiple TMDs. Therefore, mutations have the potential to greatly disturb protein structure by interfering with normal membrane insertion. To understand the possible consequences of, in particular, the *T141_L142delinsMISLISV* mutation, we compared theoretical hydropathicity plots (40) for our isolated mutations with those for wild type *psen2* and a mutation equivalent to human *N141I* (Fig 2). The *T141_L142delinsMISLISV* mutation contributes only non-polar (M, I, L, V) or, at least, uncharged, polar (S) amino acid residues (aa) to the protein structure, presumably expanding the hydrophobic stretch of aas that form TMD2. Presumably, this mutation allows overall correct membrane insertion but disrupts the conformation of the protein sufficiently to almost entirely, but not completely, destroy its γ-secretase activity (see later).

Fig 2. Predicted protein hydropathicity plots.

The blue line refers to wild type Psen2. The red lines refer to the mutants.

383 The *N140fs* mutation cannot possibly express a catalytically active γ-secretase
384 enzyme since it truncates the CDS at the start of TMD2. Thus, it lacks both the
385 aspartate residues required for the γ-secretase catalytic domain (41, 42).
386
387 **_N140fs_ transcripts are subject to nonsense-mediated decay**
388
389 Mutations creating premature termination codons (PTCs) in coding sequences
390 upstream of exon-exon junctions in spliced transcripts can result in destabilisation of
391 the transcripts through nonsense-mediated decay (NMD, reviewed by (43)). Therefore,
392 we expected that transcripts from the *T141_L142delinsMISLISV* allele might be
393 similarly stable to wild type transcripts while *N140fs* allele transcripts would show
394 decreased stability and abundance. To test this we performed dqPCR that allows direct
395 comparison of transcript abundances. We extracted total RNA from the brains of
396 6-month-old adult zebrafish, reverse transcribed this to cDNA, and then performed
397 dqPCR with primers specifically detecting the wild type or mutant alleles. The results
398 confirmed similar levels of *T141_L142delinsMISLISV* and wild type transcripts in
399 heterozygous mutant brains but levels of *N140fs* transcripts are only approximately 25%
400 of those for wild type transcripts in heterozygous mutant brains (Fig 4). The first
401 round of translation of a transcript is critical for NMD and so inhibition of translation
402 (e.g. with cycloheximide) can increase the stability of transcripts with PTCs (44, 45).
403 Cycloheximide treatment of a group of embryos heterozygous for *N140fs* caused an
404 approximately 5-fold increase in *N140fs* allele-derived transcripts but only an

405 approximately 2-fold increase in wild type transcripts (S4 File) supporting that NMD
406 destabilises *N140fs* transcripts.
407
408 **Stability of mutant allele transcripts under normoxia compared to hypoxia**
409
410 Numerous lines of evidence support that hypoxia is an important factor in the
411 development of AD (reviewed in (46)). This includes that expression of the fAD
412 genes, *PSEN1*, *PSEN2* and *APP* are upregulated under hypoxia (47-50), phenomena
413 that are conserved in zebrafish (51) despite ~420 million years of divergent evolution
414 from mammals (52). Also, hypoxia has previously been observed to inhibit NMD (53).
415 Therefore, to observe how hypoxia might affect the levels of transcripts from our
416 mutant alleles we performed dqPCR using total RNA extracted from the brains of
417 6-month-old zebrafish exposed to normoxia or hypoxia (Figs 3 and 4). This revealed
418 little effect of hypoxia on the levels of transcripts from wild type or
419 *T141_L142delinsMISLISV* alleles (Fig 3) in heterozygous fish brains (that is most
420 likely due to the young age of the fish, see Discussion) and a small, but apparently
421 statistically significant increase in the levels of *N140fs* allele transcripts (Fig 4).
422 However, we cannot distinguish whether this increase is due to induction of
423 transcription, or inhibition of NMD, or both (or other factors that could increase
424 transcript levels).
425
426 **Fig 3. *psen2* wild type and *T141_L142delinsMISLISV* allele-specific expression**

427 **(as copies per the 25 ng of total brain cDNA in each dqPCR).**

428 The expression levels of wild type *psen2* alleles in *T141_L142delinsMISLISV*/+ fish
429 (~460 copies) were significantly (p=0.0024) lower than in their wild type siblings
430 (~950 copies) under normoxia. Under hypoxia, the expression levels of wild type
431 *psen2* alleles in both *T141_L142delinsMISLISV*/+ fish (~1,000 copies) and their wild
432 type siblings (~510 copies) were up-regulated, but neither of the genotypes showed
433 statistically significant differences compared to their normoxic controls. The
434 expression levels of the *T141_L142delinsMISLISV* alleles in
435 *T141_L142delinsMISLISV*/+ fish (~520 copies under normoxia) were increased by
436 acute hypoxia (~580 copies), but without statistical significance. Means with SDs are
437 indicated.

438

439 **Fig 4. *psen2* wild type allele and *N140fs* allele-specific expression (as copies per**
440 **the 25 ng of total brain cDNA in each dqPCR).**

441 The expression levels of wild type *psen2* alleles in *N140fs*/+ fish (~860 copies) were
442 significantly (p=0.0024) lower than in their wild type siblings (~1,600 copies) under
443 normoxia. Under hypoxia, the expression levels of wild type *psen2* alleles in both
444 *N140fs*/+ fish (~860 copies) and their wild type siblings (~1,700 copies) were slightly
445 up-regulated, but not with statistical significance compared to these genotypes under
446 normoxia. The expression levels of *N140fs* alleles in *N140fs*/+ fish (~150 copies
447 under normoxia) were increased (p=0.0513) by acute hypoxia (~160 copies). Means
448 with SDs are indicated.

449

450 **Pigment phenotypes of mutation-carrying fish**

451

452 During the process of isolating mutations in *psen2*, we observed that some of the G0
453 CRISPR Cas9-injected, mosaic, mutation-carrying fish showed unique patches of
454 pigmentation loss in their skin (Fig 5A). (Four of 12 G0 fish injected with the
455 CRISPR Cas9 complex targeting the N140 codon showed this phenotype). None of
456 the F1 progeny of these fish (heterozygous for either of the mutations in *psen2*)
457 showed obvious pigmentation loss. However, when inbreeding F2 heterozygous
458 mutant fish we found that some of the F3 progeny for either the
459 *T141_L142delinsMISLISV* mutation or the *N140fs* mutation showed reduction in
460 surface melanotic pigmentation obvious to the unaided eye by one month of age.
461 Genotyping of these fish using allele-specific PCR on tail biopsies showed them to be
462 homozygous mutants, supporting that the reduced pigmentation phenotypes of the
463 mutations are recessive (see Fig 5B,C). Subsequently, we observed the development
464 of surface pigmentation with age for these fish families and saw that fish
465 heterozygous for either the *T141_L142delinsMISLISV* or *N140fs* mutation appear
466 similar to wild type fish in surface pigmentation but that homozygous
467 *T141_L142delinsMISLISV* fish have much fainter melanotic pigmentation, with many
468 faintly melanotic cells arranged in apparently normal stripes (Fig 5B). In contrast,
469 homozygous *N140fs* fish apparently lack surface melanotic stripes (although a very
470 faint impression of striping is still visible, Fig 5C). Subsequent generation of

homozygous lines of fish homozygous for both mutations showed that their reduced melanotic pigmentation phenotypes are consistent and that the mutations do not cause sterility. Since γ-secretase activity is required for melanin formation (20, 25), and *psen2* appears relatively highly expressed in melanophores (33) it is likely that *N140fs* homozygous fish lack melanin due to absence of γ-secretase activity from *psen2* while *T141_L142delinsMISLISV* homozygous fish retain low levels of *psen2*-derived γ-secretase activity.

Fig 5. Surface melanotic pigmentation phenotypes.

(A) Patches of pigmentation loss in the skin of mosaic mutant G0 fish.

(B) *T141_L142delinsMISLISV* mutants and +/+ sibling fish.

(C) *N140fs* mutants and +/+ sibling fish.

(D) No gross melanotic pigmentation phenotype was observed in *N140fs* homozygous embryos at 50 hpf.

When stripes of melanotic pigmentation were visible in heterozygous or homozygous mutant fish, we did not observe obvious differences in the overall pattern of striping between these and wild type fish (data not shown).

The intracellular distribution of pigment also appeared to change with age in the skin melanophores of *T141_L142delinsMISLISV* homozygous fish. At two months of age pigment appeared evenly distributed in these cells but excluded from their central, presumably nuclear, regions (Fig 5B). However, by six months of age, the pigment

493 appeared concentrated at the centre of cells and was, presumably, perinuclear. The
494 density of pigment formation in heterozygous and wild type fish made it difficult to
495 see whether a similar phenomenon was also occurring in those.
496
497 Curiously, the *N140fs* homozygous fish lacking surface melanotic pigmentation
498 retained strong melanotic pigmentation in their retinal pigmented epithelium. This is
499 obvious as the dark eyes of the fish shown in Fig 5C and was confirmed by dissection
500 of these eyes (not shown). Also, all the 48 hpf larval *N140fs* homozygous progeny of
501 homozygous parents showed abundant surface melanophores that cannot be due to
502 maternal inheritance of wild type *psen2* function (Fig 5D). Thus, the dependence of
503 zebrafish adult skin melanotic pigmentation on *psen2* function is both cell type- and
504 age-specific.
505
506 ## Discussion
507
508 Our attempts at generation of point mutations in the zebrafish *psen2* gene by HDR
509 were unsuccessful. However, we did succeed in identifying two mutations (formed by
510 the NHEJ pathway) that may prove useful in analysing the role of the human *PSEN2*
511 gene in familial Alzheimer's disease; an in-frame mutation,
512 *T141_L142delinsMISLISV*, and a frame-shift mutation, *N140fs*. While the CRISPR
513 Cas9 system can produce off-target effects (54) these are unlikely to have influenced
514 out results since use of this system in zebrafish requires outbreeding of fish that

typically segregates away second-site mutations (other than those tightly linked to the target mutation site). Also, the severity of the phenotypic effects observed corresponds to the severity of the effects of the mutations on the structure of the putative encoded proteins. It is also unlikely that two off-target mutation events would both affect pigmentation. Lastly, the effects of mutations in zebrafish *psen2* upon pigmentation are consistent with what is known about the subcellular localization of PSEN2 protein in mammalian systems (10).

The in-frame mutation *T141_L142delinsMISLISV* is an indel mutation altering two codons and inserting an additional 5 codons. Although this mutation changes the length of the protein coding sequence, the predicted protein hydropathicity plot of the putative mutant protein (Fig 2) supports that the mutation does not completely destroy the transmembrane structure of Psen2. Since most of the fAD mutations in human *PSEN2* are in-frame mutations that may change hydropathicity without destroying the overall transmembrane structure of the protein (4), the *T141_L142delinsMISLISV* mutation would appear to be more fAD-like than null.

The frame-shift mutation *N140fs* was caused by a deletion of 7 nucleotides and results in a PTC at the 142nd codon position. This mutation causes truncation of the coding sequence at the upstream end of TMD2 of zebrafish Psen2. The first two TMDs of human PSEN2 are thought to be necessary for ER localisation (11). Since coding sequence truncation occurs at the upstream end of TMD2, if this mutant allele

expressed a protein, it would most likely not be able to form TMD structures for ER localization. Neither could it possibly have γ-secretase activity since it lacks the aspartate residues required (41, 42). Moreover, since dqPCR showed that the levels of *N140fs* transcripts are only approximately 25% of those for wild type transcripts in heterozygous mutant brains, *N140fs* expression appears limited by NMD (a fact supported by the ~5-fold increased N140fs transcript level in the presence of the translation inhibitor, cycloheximide (S4 File). Our previous work has shown that zebrafish *psen2* does not express a truncated isoform equivalent to the PS2V isoform of human *PSEN2* (39) and that a PS2V-like truncation of zebrafish Psen2 does not have PS2V-like activity (55). (Instead a PS2V-like function is expressed from zebrafish *psen1* (55)). Therefore, *N140fs* most likely represents a true null (or severely hypomorphic) allele of zebrafish *psen2*, unlike another frameshift mutation, *S4Ter*, that we recently analysed and that shows grossly normal adult pigmentation (Jiang et al., manuscript submitted).

There is a considerable weight of evidence supporting the importance of hypoxia in the development of AD (reviewed by (56)) and zebrafish represent a very versatile system for investigating the effects of hypoxia (39, 51, 55). In human cells, expression of the fAD genes *APP*, *PSEN1* and *PSEN2* genes can be upregulated by hypoxia (51) and we previously showed that this phenomenon has been conserved during the nearly half a billion years since the divergence of the zebrafish and human evolutionary lineages (51). In that earlier paper we saw nearly a two-fold increase in

559 zebrafish brain *psen2* mRNA levels under hypoxia compared to normoxia while, in
560 this work, no significant differences were seen (except for *N140fs* allele transcripts
561 where hypoxia may be inhibiting NMD (53)). Upon checking our laboratory records
562 we found that the fish used in the earlier publication were around 12 months old
563 compared to the six months of age in this work. In other, yet unpublished work we
564 have observed that differences in adult age make very significant differences to brain
565 transcriptional responses to hypoxia with young adult fish showing the mildest
566 responses (Newman et al. unpublished results).
567
568 In previous research we showed that blockage of *psen2* function using morpholino
569 antisense nucleotides injected into zebrafish zygotes increases the number of DoLA
570 neurons at 24 hpf (57). Despite the evidence that the *N140fs* mutation is null, we did
571 not see increased DoLA neuron numbers in *N140fs* homozygous embryos at 24 hpf
572 (See S3 Files for experiment description and data). The observation of differing
573 developmental phenotypes from decreased gene function due to mutation or
574 morpholino injection is a common occurrence (58). It is thought to be due to the
575 phenomenon of “genetic compensation” whereby only decreased gene function
576 through mutation, (and not by morpholino injection), causes compensatory
577 upregulation of other genes with similar activities (59). It is likely that genetic
578 compensation is causing the lack of response of DoLA neuron number to the *N140fs*
579 mutation. An alternative explanation would be a maternal contribution of wild type
580 *psen2* activity from the heterozygous *N140fs* mother of the embryos examined.

Further experimentation such as blockage of *psen1* translation by morpholino injection into *N140fs* homozygous embryos or analysis of DoLA numbers in *N140fs* homozygous embryos from homozygous parents might resolve this question.

The visually striking surface pigmentation pattern of zebrafish and the genetic utility of this organism has made it a focus for research on the genetic control of pigment formation (60), pigment cell differentiation (61), and surface pigmentation pattern formation (62). Skin pigmentation pattern is severely affected in adult fish homozygous for the mutation *T141_L142delinsMISLISV*. These fish show surface melanotic stripes that appear approximately the same width as in wild type fish but are much fainter. Closer examination of these stripes at 6 months of age reveals cells with vestigial, and likely perinuclear, pigment. The number of cells is not obviously affected, only the pigmentation they show. Thus, loss of *psen2* function does not appear to affect melanophore viability (although, in an animal as highly regenerative as the zebrafish, further tests would be required to conclude this with certainty). By extrapolation it appears likely that *N140fs* homozygous adult fish still possess skin melanophores but that these lack melanin. The retention of some adult skin melanin formation in *T141_L142delinsMISLISV* homozygotes but not *N140fs* homozygotes, and the roles played in melanosome formation and function particularly by PSEN2-derived γ-secretase activity (10, 28), support that *T141_L142delinsMISLISV* mutant Psen2 protein molecules retain some level of γ-secretase activity. (Indeed, Sannerud et al (10) observed that loss of *PSEN2* activity in a human melanoma cell

603 line, MNT1, greatly reduced γ-secretase cleavage of tyrosinase-related protein (TRP1)
604 and premelanosome protein (PMEL) that are important for melanosome function.)
605 This supports that the *T141_L142delinsMISLISV* mutation of zebrafish Psen2 does not
606 seriously disrupt the protein's overall pattern of folding for membrane insertion, but
607 does distort its conformation sufficiently to reduce γ-secretase activity. Partial loss of
608 γ-secretase activity is a commonly observed characteristic of fAD-like mutations in
609 *PRESENILIN* genes. For example, mouse skin completely lacking expression of wild
610 type *Psen1* and *Psen2* genes but with a single knock-in M146V fAD-like allele of
611 *Psen1* show lighter skin and coat colour than similar mice possessing a single wild
612 type allele of *Psen1* (20). These data, and the fact that the *T141_L142delinsMISLISV*
613 mutation obeys the "fAD mutation reading frame preservation rule" (7), support that
614 this mutation should be investigated for its utility in zebrafish-based fAD research.
615
616 Intriguingly, only the melanotic pigmentation of adult zebrafish skin is dependent on
617 *psen2* function while larvae and cells of the retinal pigmented epithelium do not show
618 this dependency. In mammalian systems, most melanin synthesis in the retinal
619 pigmented epithelium occurs during embryogenesis (63). However, maternal
620 inheritance of wild type *psen2* mRNA acting during zebrafish embryo formation
621 cannot explain the pigmented melanophores of larvae or the pigmentation in adult
622 retinas of *N140fs* homozygotes since this pigmentation is observed in the progeny of
623 homozygous mutant parents. The pigmentation likely indicates that the Psen1 protein
624 (or, possibly, another protein with γ-secretase-like activity (7)) contributes to normal

melanosome formation in the melanophores of embryos/larvae and in the retinal pigmented epithelium of zebrafish. That different PRESENILIN proteins might contribute differentially to melanosome formation in different cells or in the same cell type at different ages is a level of developmental complexity that has not previously been appreciated. Alternatively, the skin melanophores of adult fish might, for some unknown reason, be incapable of genetic compensation (e.g. upregulation of *psen1* activity when *psen2* activity is lost through mutation). The possibility of cell type-specificity of genetic compensation has also not previously been considered. The lack of an obvious larval pigmentation phenotype explains why *psen2* was not identified by the large mutation screens for developmental phenotypes conducted by the laboratories of Christiane Nüsslein-Volhard (64) and Wolfgang Driever (65) and published in 1996.

In conclusion, we have generated in zebrafish an EOfAD-like mutation, *T141_L142delinsMISLISV*, and an apparent null, loss-of-function mutation *N140fs*. Since none of the over 200 human fAD mutations in *PSEN1* and *PSEN2* are obviously null alleles, these two zebrafish mutations may prove useful for defining the brain gene regulatory and other molecular changes that are particular to fAD mutations in the *PRESENILIN* genes. Our future work will use these and other zebrafish mutation models to dissect how fAD-like mutations contribute to Alzheimer's disease. Also, Higdon et al (66) showed that it is possible to use cell-sorting techniques on disassociated zebrafish embryos to isolate relatively pure populations of their different

pigment cells types. These were subsequently characterised transcriptomically. Extension of these technologies to larval, retinal, and adult tissues would allow more detailed analysis of the differences between the melanotic cells of these stages and tissues to determine why they are differentially dependent on *psen2* activity for melanosome formation and function.

Acknowledgments

The authors wish to thank Seyyed Hani Moussavi Nik for kind assistance in adjusting the conditions for the dqPCR.

References

1. alz.co.uk. World Alzheimer Report 2014: Dementia and Risk Reduction. Alzheimer's Disease International; 2014.
2. Campion D, Dumanchin C, Hannequin D, Dubois B, Belliard S, Puel M, et al. Early-Onset Autosomal Dominant Alzheimer Disease: Prevalence, Genetic Heterogeneity, and Mutation Spectrum. The American Journal of Human Genetics.65(3):664-70.
3. Guerreiro R, Hardy J. Genetics of Alzheimer's disease. Neurotherapeutics. 2014;11(4):732-7.
4. Jayadev S, Leverenz JB, Steinbart E, Stahl J, Klunk W, Yu CE, et al. Alzheimer's disease phenotypes and genotypes associated with mutations in presenilin 2. Brain. 2010;133(Pt 4):1143-54.
5. Scherzer CR, Offe K, Gearing M, Rees HD, Fang G, Heilman CJ, et al. Loss of apolipoprotein E receptor LR11 in Alzheimer disease. Arch Neurol. 2004;61(8):1200-5.
6. Pottier C, Hannequin D, Coutant S, Rovelet-Lecrux A, Wallon D, Rousseau S, et al. High frequency of potentially pathogenic SORL1 mutations in autosomal dominant early-onset Alzheimer disease. Mol Psychiatry. 2012;17(9):875-9.
7. Jayne T, Newman M, Verdile G, Sutherland G, Munch G, Musgrave I, et al. Evidence For and Against a Pathogenic Role of Reduced gamma-Secretase Activity in Familial Alzheimer's Disease. J Alzheimers Dis. 2016;52(3):781-99.
8. Jumpertz T, Rennhack A, Ness J, Baches S, Pietrzik CU, Bulic B, et al. Presenilin is the molecular target of acidic gamma-secretase modulators in living cells. PLoS ONE. 2012;7(1):6.
9. Area-Gomez E, de Groof AJ, Boldogh I, Bird TD, Gibson GE, Koehler CM, et al. Presenilins are enriched in endoplasmic reticulum membranes associated with mitochondria. Am J Pathol.

679 2009;175(5):1810-6.
680 10. Sannerud R, Esselens C, Ejsmont P, Mattera R, Rochin L, Tharkeshwar AK, et al. Restricted
681 Location of PSEN2/gamma-Secretase Determines Substrate Specificity and Generates an Intracellular
682 Abeta Pool. Cell. 2016;166(1):193-208.
683 11. Tomita T, Tokuhiro S, Hashimoto T, Aiba K, Saido TC, Maruyama K, et al. Molecular dissection of
684 domains in mutant presenilin 2 that mediate overproduction of amyloidogenic forms of amyloid beta
685 peptides. Inability of truncated forms of PS2 with familial Alzheimer's disease mutation to increase
686 secretion of Abeta42. J Biol Chem. 1998;273(33):21153-60.
687 12. Bissig C, Rochin L, van Niel G. PMEL Amyloid Fibril Formation: The Bright Steps of Pigmentation.
688 Int J Mol Sci. 2016;17(9).
689 13. Schraermeyer U, Peters S, Thumann G, Kociok N, Heimann K. Melanin granules of retinal pigment
690 epithelium are connected with the lysosomal degradation pathway. Exp Eye Res. 1999;68(2):237-45.
691 14. Wasmeier C, Hume AN, Bolasco G, Seabra MC. Melanosomes at a glance. J Cell Sci. 2008;121(Pt
692 24):3995-9.
693 15. Levy-Lahad E, Wasco W, Poorkaj P, Romano DM, Oshima J, Pettingell WH, et al. Candidate gene
694 for the chromosome 1 familial Alzheimer's disease locus. Science. 1995;269(5226):973-7.
695 16. Hardy J. Amyloid, the presenilins and Alzheimer's disease. Trends in Neurosciences. 1997
696 1997/05/01/;20(4):154-9.
697 17. Adzhubei IA, Schmidt S, Peshkin L, Ramensky VE, Gerasimova A, Bork P, et al. A method and
698 server for predicting damaging missense mutations: Nat Methods. 2010 Apr;7(4):248-9. doi:
699 10.1038/nmeth0410-248.
700 18. Tomita T, Maruyama K, Saido TC, Kume H, Shinozaki K, Tokuhiro S, et al. The presenilin 2 mutation
701 (N141I) linked to familial Alzheimer disease (Volga German families) increases the secretion of amyloid
702 β protein ending at the 42nd (or 43rd) residue. Proceedings of the National Academy of Sciences.
703 1997 March 4, 1997;94(5):2025-30.
704 19. Toda T, Noda Y, Ito G, Maeda M, Shimizu T. Presenilin-2 Mutation Causes Early Amyloid
705 Accumulation and Memory Impairment in a Transgenic Mouse Model of Alzheimer's Disease. Journal
706 of Biomedicine and Biotechnology. 2011;2011.
707 20. Wang R, Tang P, Wang P, Boissy RE, Zheng H. Regulation of tyrosinase trafficking and processing
708 by presenilins: partial loss of function by familial Alzheimer's disease mutation. Proc Natl Acad Sci U S
709 A. 2006;103(2):353-8.
710 21. Tief K, Hahne M, Schmidt A, Beermann F. Tyrosinase, the key enzyme in melanin synthesis, is
711 expressed in murine brain. Eur J Biochem. 1996;241(1):12-6.
712 22. del Marmol V, Beermann F. Tyrosinase and related proteins in mammalian pigmentation. FEBS
713 Lett. 1996;381(3):165-8.
714 23. Vetrivel KS, Zhang Y-w, Xu H, Thinakaran G. Pathological and physiological functions of presenilins.
715 Molecular Neurodegeneration. [journal article]. 2006 June 12;1(1):4.
716 24. Watt B, van Niel G, Raposo G, Marks MS. PMEL: a pigment cell-specific model for functional
717 amyloid formation. Pigment Cell Melanoma Res. 2013;26(3):300-15.
718 25. Kummer MP, Maruyama H, Huelsmann C, Baches S, Weggen S, Koo EH. Formation of Pmel17
719 amyloid is regulated by juxtamembrane metalloproteinase cleavage, and the resulting C-terminal
720 fragment is a substrate for gamma-secretase. J Biol Chem. 2009;284(4):2296-306.
721 26. Raposo G, Marks MS. Melanosomes--dark organelles enlighten endosomal membrane transport.
722 Nat Rev Mol Cell Biol. 2007;8(10):786-97.

723 27. Fowler DM, Koulov AV, Alory-Jost C, Marks MS, Balch WE, Kelly JW. Functional Amyloid
724 Formation within Mammalian Tissue. PLoS Biology. 2005;4(1):e6.
725 28. Rochin L, Hurbain I, Serneels L, Fort C, Watt B, Leblanc P, et al. BACE2 processes PMEL to form the
726 melanosome amyloid matrix in pigment cells. Proc Natl Acad Sci U S A. 2013;110(26):10658-63.
727 29. Hin N, Newman M, Kaslin J, Douek AM, Lumsden A, Zhou X-F, et al. Accelerated brain aging
728 towards transcriptional inversion in a zebrafish model of familial Alzheimer's disease. bioRxiv.
729 [10.1101/262162]. 2018.
730 30. Postlethwait JH, Woods IG, Ngo-Hazelett P, Yan Y-L, Kelly PD, Chu F, et al. Zebrafish Comparative
731 Genomics and the Origins of Vertebrate Chromosomes. Genome Research. 2000 December 1,
732 2000;10(12):1890-902.
733 31. Ravi V, Venkatesh B. Rapidly evolving fish genomes and teleost diversity. Current Opinion in
734 Genetics & Development. 2008;18(6):544-50.
735 32. Leimer U, Lun K, Romig H, Walter J, Grünberg J, Brand M, et al. Zebrafish (Danio rerio) Presenilin
736 Promotes Aberrant Amyloid β-Peptide Production and Requires a Critical Aspartate Residue for Its
737 Function in Amyloidogenesis†. Biochemistry. 1999 1999/10/01;38(41):13602-9.
738 33. Groth C, Nornes S, McCarty R, Tamme R, Lardelli M. Identification of a second presenilin gene in
739 zebrafish with similarity to the human Alzheimer's disease gene presenilin2. Dev Genes Evol. 2002
740 2002/11/01;212(10):486-90.
741 34. Bassett A, Liu J-L. CRISPR/Cas9 mediated genome engineering in Drosophila. Methods. 2014
742 2014/09/01/;69(2):128-36.
743 35. Bassett AR, Liu J-L. CRISPR/Cas9 and Genome Editing in Drosophila. Journal of Genetics and
744 Genomics. 2014 2014/01/20/;41(1):7-19.
745 36. Meeker ND, Hutchinson SA, Ho L, Trede NS. Method for isolation of PCR-ready genomic DNA
746 from zebrafish tissues. Biotechniques. 2007;43(5):614.
747 37. Bibikova M, Golic M, Golic KG, Carroll D. Targeted chromosomal cleavage and mutagenesis in
748 Drosophila using zinc-finger nucleases. Genetics. 2002;161(3):1169-75.
749 38. Babon JJ, McKenzie M, Cotton RGH. The use of resolvases T4 endonuclease VII and T7
750 endonuclease I in mutation detection. Molecular Biotechnology. [journal article]. 2003 January
751 01;23(1):73-81.
752 39. Moussavi Nik SH, Newman M, Lardelli M. The response of HMGA1 to changes in oxygen
753 availability is evolutionarily conserved. Exp Cell Res. 2011;317(11):1503-12.
754 40. Gasteiger E, Hoogland C, Gattiker A, Wilkins MR, Appel RD, Bairoch A. Protein identification and
755 analysis tools on the ExPASy server. The proteomics protocols handbook: Springer; 2005. p. 571-607.
756 41. Fraering PC. Structural and Functional Determinants of gamma-Secretase, an Intramembrane
757 Protease Implicated in Alzheimer's Disease. Curr Genomics. 2007;8(8):531-49.
758 42. Wolfe MS, Xia W, Ostaszewski BL, Diehl TS, Kimberly WT, Selkoe DJ. Two transmembrane
759 aspartates in presenilin-1 required for presenilin endoproteolysis and gamma-secretase activity.
760 Nature. 1999;398(6727):513-7.
761 43. Chang YF, Imam JS, Wilkinson MF. The nonsense-mediated decay RNA surveillance pathway.
762 Annu Rev Biochem. 2007;76:51-74.
763 44. Carter MS, Doskow J, Morris P, Li S, Nhim RP, Sandstedt S, et al. A regulatory mechanism that
764 detects premature nonsense codons in T-cell receptor transcripts in vivo is reversed by protein
765 synthesis inhibitors in vitro. J Biol Chem. 1995;270(48):28995-9003.
766 45. Hurt JA, Robertson AD, Burge CB. Global analyses of UPF1 binding and function reveal expanded

767 scope of nonsense-mediated mRNA decay. Genome Res. 2013;23(10):1636-50.
768 46. Salminen A, Kauppinen A, Kaarniranta K. Hypoxia/ischemia activate processing of Amyloid
769 Precursor Protein: impact of vascular dysfunction in the pathogenesis of Alzheimer's disease. Journal
770 of Neurochemistry. 2017;140(4):536-49.
771 47. Nishikawa A, Manabe T, Katayama T, Kudo T, Matsuzaki S, Yanagita T, et al. Novel function of PS2V:
772 change in conformation of tau proteins. Biochem Biophys Res Commun. 2004;318(2):435-8.
773 48. De Gasperi R, Sosa MA, Dracheva S, Elder GA. Presenilin-1 regulates induction of hypoxia
774 inducible factor-1alpha: altered activation by a mutation associated with familial Alzheimer's disease.
775 Mol Neurodegener. 2010;5(38):1750-326.
776 49. Sato N, Hori O, Yamaguchi A, Lambert JC, Chartier-Harlin MC, Robinson PA, et al. A novel
777 presenilin-2 splice variant in human Alzheimer's disease brain tissue. J Neurochem.
778 1999;72(6):2498-505.
779 50. Zhang X, Zhou K, Wang R, Cui J, Lipton SA, Liao F-F, et al. Hypoxia-inducible Factor 1α
780 (HIF-1α)-mediated Hypoxia Increases BACE1 Expression and β-Amyloid Generation. Journal of
781 Biological Chemistry. 2007 April 13, 2007;282(15):10873-80.
782 51. Moussavi Nik SH, Wilson L, Newman M, Croft K, Mori TA, Musgrave I, et al. The
783 BACE1-PSEN-AbetaPP regulatory axis has an ancient role in response to low oxygen/oxidative stress. J
784 Alzheimers Dis. 2012;28(3):515-30.
785 52. Detrich III HW, Zon LI, Westerfield M. Essential zebrafish methods: Genetics and genomics:
786 Academic Press; 2009.
787 53. Gardner LB. Hypoxic Inhibition of Nonsense-Mediated RNA Decay Regulates Gene Expression and
788 the Integrated Stress Response. Molecular and Cellular Biology. 2008 June 1, 2008;28(11):3729-41.
789 54. Zhang X-H, Tee LY, Wang X-G, Huang Q-S, Yang S-H. Off-target Effects in CRISPR/Cas9-mediated
790 Genome Engineering. Molecular Therapy - Nucleic Acids. 2015 2015/01/01/;4:e264.
791 55. Moussavi Nik SH, Newman M, Wilson L, Ebrahimie E, Wells S, Musgrave I, et al. Alzheimer's
792 disease-related peptide PS2V plays ancient, conserved roles in suppression of the unfolded protein
793 response under hypoxia and stimulation of gamma-secretase activity. Hum Mol Genet. 2015;26.
794 56. Love S, Miners JS. Cerebral Hypoperfusion and the Energy Deficit in Alzheimer's Disease. Brain
795 Pathol. 2016;26(5):607-17.
796 57. Nornes S, Newman M, Wells S, Verdile G, Martins RN, Lardelli M. Independent and cooperative
797 action of Psen2 with Psen1 in zebrafish embryos. Experimental Cell Research. 2009
798 2009/10/01/;315(16):2791-801.
799 58. Kok FO, Shin M, Ni CW, Gupta A, Grosse AS, van Impel A, et al. Reverse genetic screening reveals
800 poor correlation between morpholino-induced and mutant phenotypes in zebrafish. Dev Cell.
801 2015;32(1):97-108.
802 59. Rossi A, Kontarakis Z, Gerri C, Nolte H, Hölper S, Krüger M, et al. Genetic compensation induced
803 by deleterious mutations but not gene knockdowns. Nature. 2015;524:230.
804 60. Navarro RE, Ramos-Balderas JL, Guerrero I, Pelcastre V, Maldonado E. Pigment dilution mutants
805 from fish models with connection to lysosome-related organelles and vesicular traffic genes. Zebrafish.
806 2008;5(4):309-18.
807 61. Quigley IK, Parichy DM. Pigment pattern formation in zebrafish: a model for developmental
808 genetics and the evolution of form. Microsc Res Tech. 2002;58(6):442-55.
809 62. Irion U, Singh AP, Nusslein-Volhard C. The Developmental Genetics of Vertebrate Color Pattern
810 Formation: Lessons from Zebrafish. Curr Top Dev Biol. 2016;117:141-69.

63. Lopes VS, Wasmeier C, Seabra MC, Futter CE. Melanosome maturation defect in Rab38-deficient retinal pigment epithelium results in instability of immature melanosomes during transient melanogenesis. Mol Biol Cell. 2007;18(10):3914-27.

64. Kelsh RN, Brand M, Jiang YJ, Heisenberg CP, Lin S, Haffter P, et al. Zebrafish pigmentation mutations and the processes of neural crest development. Development. 1996;123:369-89.

65. Driever W, Solnica-Krezel L, Schier AF, Neuhauss SC, Malicki J, Stemple DL, et al. A genetic screen for mutations affecting embryogenesis in zebrafish. Development. 1996;123:37-46.

66. Higdon CW, Mitra RD, Johnson SL. Gene expression analysis of zebrafish melanocytes, iridophores, and retinal pigmented epithelium reveals indicators of biological function and developmental origin. PLoS ONE. 2013;8(7).

Supporting information

S1 Fig. T7 endonuclease assays and mutation-specific PCRs for embryos at 24 hpf.

(A) T7 endonuclease I assay for testing the cleavage activity of the CRISPR/Cas9 system.

(B) "*N140I*" allele-detection PCR for testing of CRISPR/Cas9 plus "N140I oligo" co-injected TU embryos. 10 embryos from each injection batch were pooled for these tests. Both batches of the injected TU embryos showed positive signals in the "N140I" allele-detection PCR. Therefore, some of these "N140I oligo" injected TU embryos may have carried the "N140I" allele in the genomes of some cells.

(C) "*V147I*" allele-detection PCR for testing the CRISPR/Cas9 plus "V147I oligo" injected TU embryos. 10 embryos from each batch were pooled for these tests. Both batches of the injected TU embryos showed positive signals from the "*V147I*" allele-detection PCR. Therefore, some of these "V147I oligo" injected TU embryos may have carried the "*V147I*" allele in the genomes of some cells.

(D) T7 endonuclease I assay for detecting random mutations at the CRISPR/Cas9 target site in the F1 progeny. Tail-clip biopsies from 46 of the F1 progeny from the CRISPR/Cas9 plus "V147I oligo" injected mosaic G0 fish were tested using the T7 endonuclease I assay to screen for the presence of cells with mutations at the target site. Only 5 fish showed cleavage patterns indicating the presence of mutations.

S2 Fig. Mutation-specific PCR tests of G0 and F1 fish.

(A) "*N140I*" allele-specific detection PCRs on tail-clip biopsies from G0 fish. Twelve G0 fish (120 in total) showed positive signals in the "N140I" allele-specific detection PCR.

(B) "*N140I*" allele-specific detection PCRs from F1 embryos of the G0 mosaic fish showing "*N140I*" allele-positive signals. 10 F1 embryos at 24 hpf from each "*N140I*" allele-carrying G0 fish were pooled for testing. The F1 progeny from one "*N140I*" allele-carrying G0 fish showed a signal at ~400 bp, which may result from imperfect incorporation of the "N140I oligo" sequence into the target site of the CRISPR/Cas9 system.

(C) "*V147I*" allele-specific PCRs from F1 embryos of the G0 mosaic fish showing "*V147I*" allele-positive signals. 10 F1 embryos at 24 hpf from each "*V147I*" allele carrying G0 fish were pooled for testing. The F1 progeny from one of the "*V147I*" allele-carrying G0 fish showed the same positive signal as the injected G0 embryos.

(D) "*V147I*" allele-specific detection PCR from tail-clip biopsies of F1 fish. Two out of twelve tested F1 fish (raised from the positive batch of embryos observed above in

D) showed positive signals, indicating they might carry the desired "*V147I*" allele.

(E) "*V147I*" allele-specific detection PCR using the same forward primer as in (E) but a different reverse primer binding farther downstream in *psen2* DNA. While the pooled F1 embryos still gave a positive signal, the two F1 fish no longer showed a positive signal using this PCR, revealing that the previously seen positive signals (in E) were artefacts.

S3 Fig. DoLA neuron numbers.

DoLA neuron numbers in wild type and *N140fs* mutant embryos as revealed by *in situ* hybridisation against *tbx16* transcripts.

S4 Fig. dqPCRs detecting wild type and mutant alleles in *N140fs*/+ embryos at 50 hpf after two hours of cycloheximide treatment relative to untreated embryos.

(A) In a 20% polyacrylamide gel, amplification of cDNA fragments spanning the mutation (7 nucleotides shorter than wild type) was only observed in the CHX-treated group, while only one higher molecular weight band (from the wild type allele) was observed in the non-treated group. This supports that NMD is destabilising the mutant transcript in heterozygous embryos.

(B) In dqPCR, both the wild type *psen2* allele and the *N140fs* allele were observed to be upregulated after the CHX-treatment. The fold change (FC) of the upregulation of the *N140fs* allele transcripts (FC=5.601) was significantly higher than that for the wild type *psen2* allele transcripts (FC=2.373).

S1 Table. Allele-specific transcript quantification in six month old *T141_L142delinsMISLISV*/+ and wild type sibling brains. Copies per 25ng of total brain cDNA (assuming complete reverse transcription of total brain RNA).

S2 Table. Allele-specific transcript quantification in six month old *N140fs*/+ fish and wild type sibling brains. Copies per 25ng of total brain cDNA (assuming complete reverse transcription of total brain RNA).

S3 Table. *In situ* hybridization against *tbx16* transcripts in DoLA neurons.

S4 Table. Allele-specific expression analysis on the *N140fs*/+ embryos (non-treated and CHX–treated) at 50 hpf in 25ng of total embryo cDNA. Copies per 25ng (assuming complete reverse transcription of total RNA).

S1 File. Mutation screening and breeding.

S2 File. dqPCR results for allele-specific transcript quantification in six month old brains.

S3 File. *In situ* transcript hybridization analysis of DoLA neuron number.

905 **S4 File. Cycloheximide treatment of *N140fs*/+ embryos at 48-50 hpf.**

A

psen2 wildtype

cDNA TCAGTGGGCCAGCGTCTGCTGAATTCGGTGCTCAAC----------ACTCTGGTCATGATCAGTGTGATTGTCTTCATGACCA
Protein S V G Q R L L N S V L N---------- T L V M I S V I V F M T

psen2 T141_L142delinsMISLISV

cDNA TCAGTGGGCCAGCGTCTGCTGAATTCGGTGCTCAACATGATCAGTCTGATCAGTGTGGTCATGATCAGTGTGATTGTCTTCATGACCA
Protein S V G Q R L L N S V L N M I S L I S V V M I S V I V F M T

psen2 N140fs

cDNA TCAGTGGGCCAGCGTCTGCTGAATTCGGTGCTC---------------TGGTCATGATCAGTGTGATTGTCTTCATGACCA
Protein S V G Q R L L N S V L--------------- W S * S V * L S S * P

B

psen2 wildtype

psen2 N140I

psen2 T141_L142delinsMISLISV

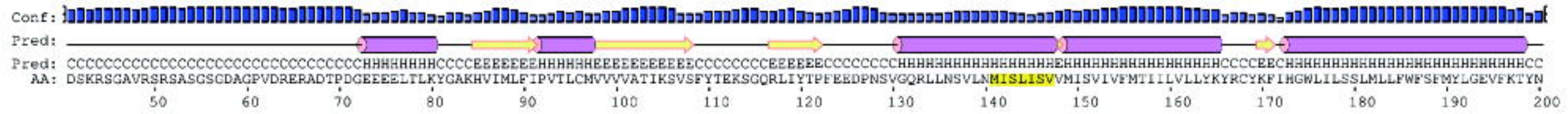

psen2 N140fs

A

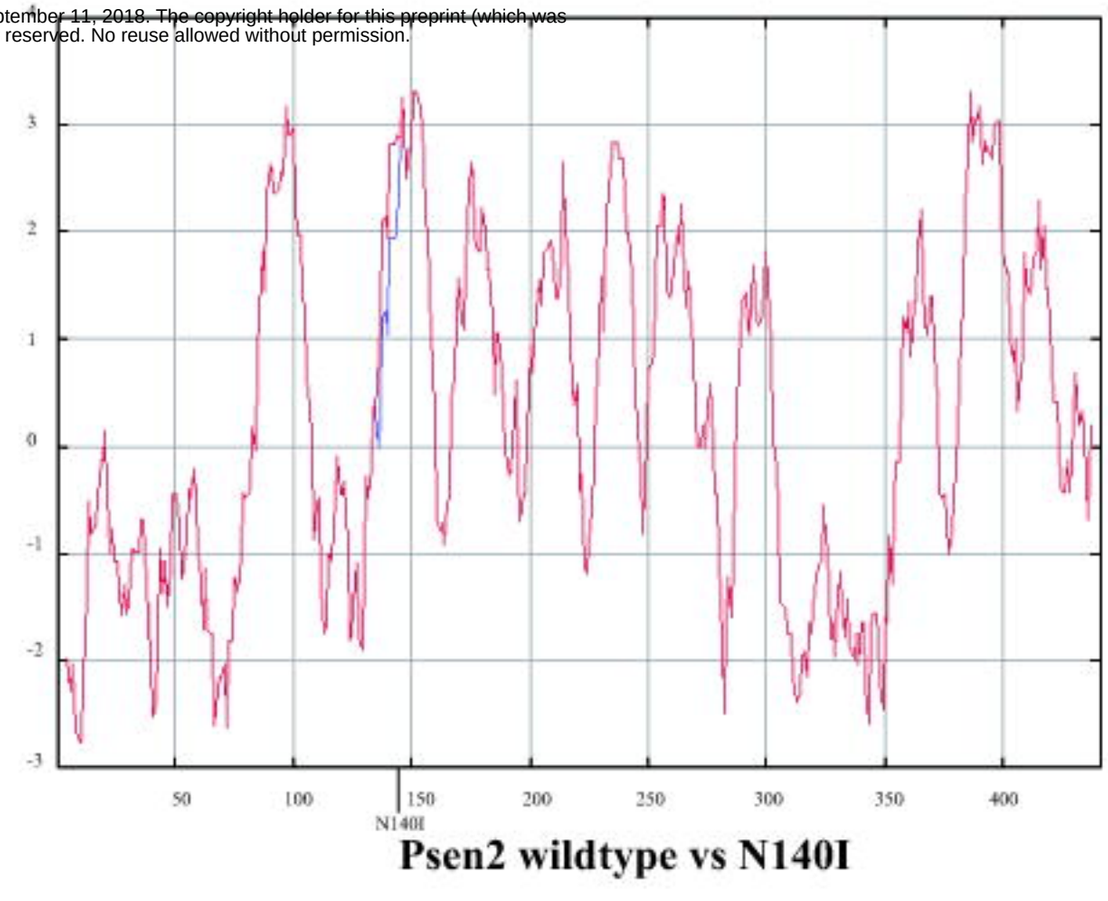

Psen2 wildtype vs N140I

B

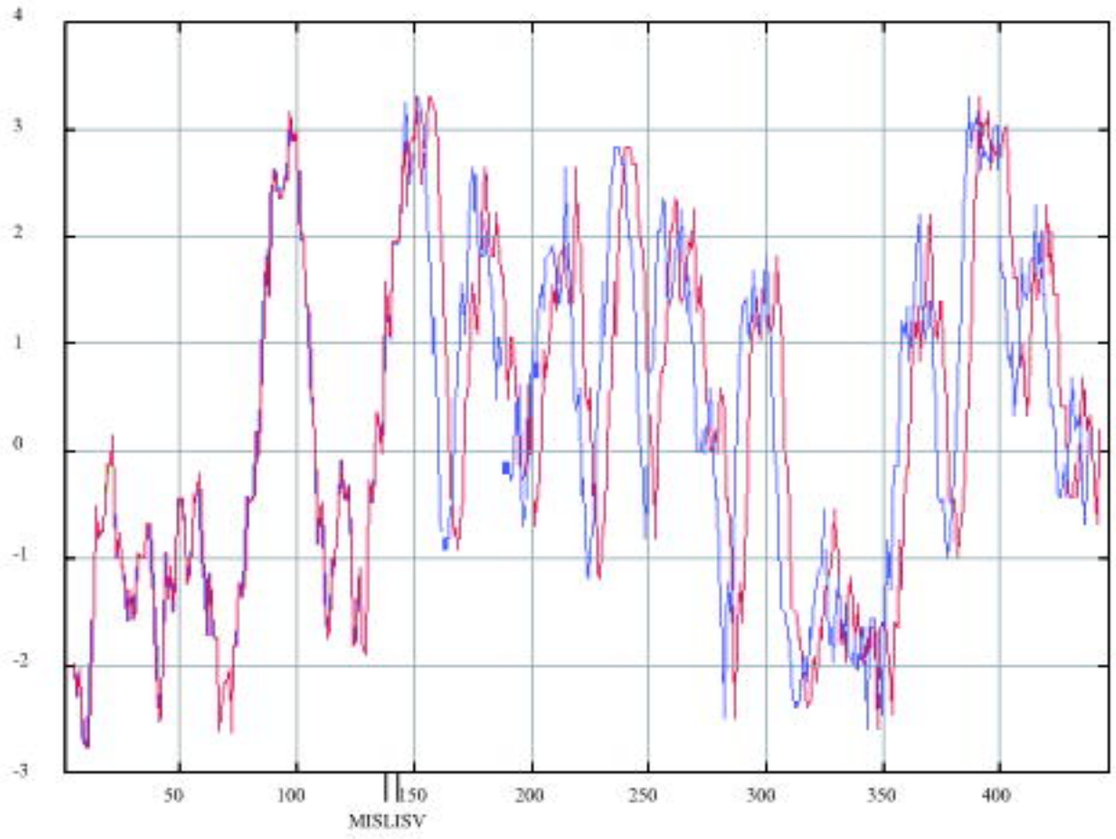

Psen2 wildtype vs T141_L142delinsMISLISV

C

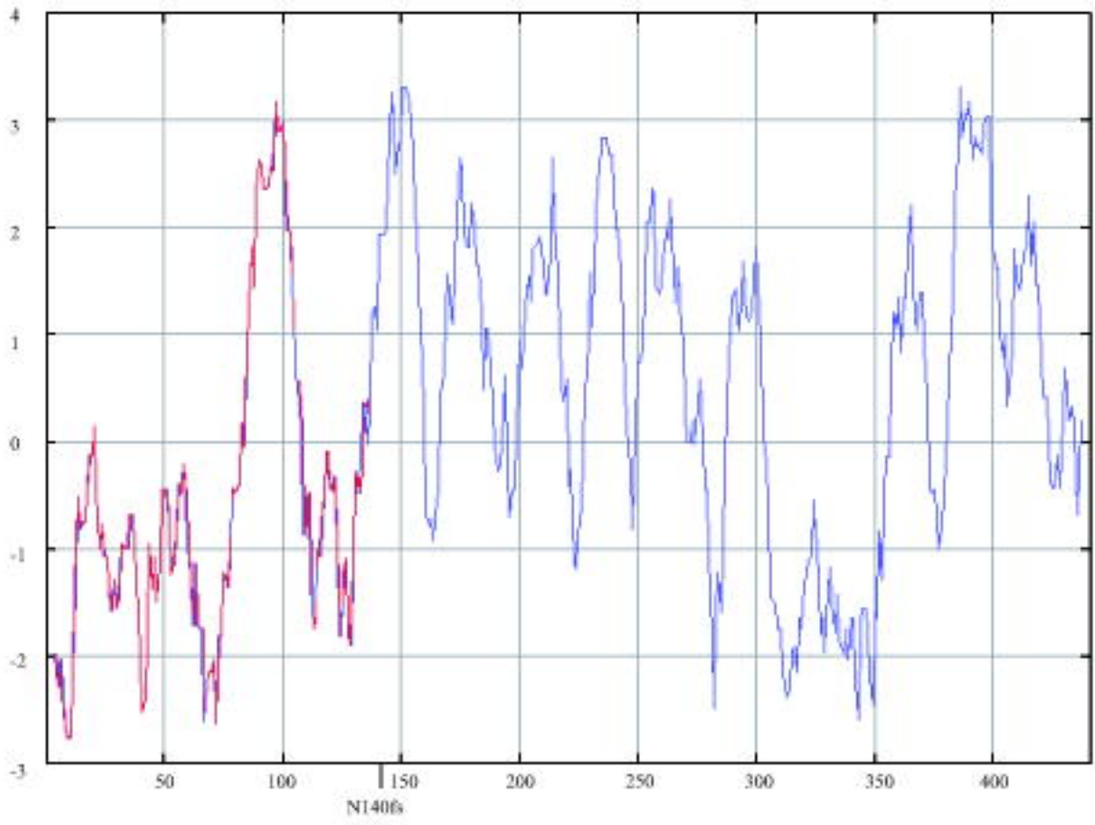

Psen2 wildtype vs N140fs

***psen2* wild type allele and *T141_L142delinsMISLISV* allele-specific expression in 25 ng total brain cDNA**

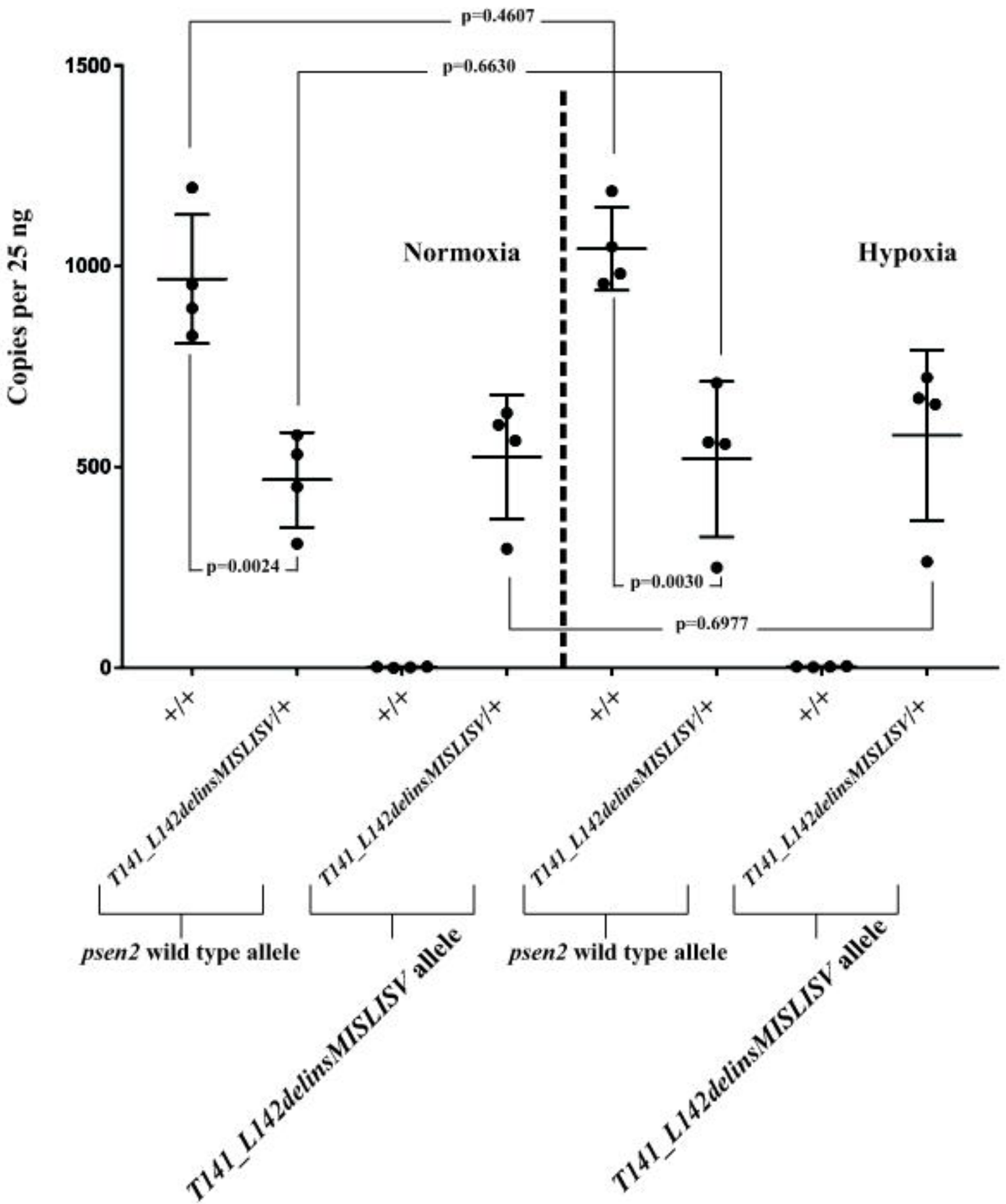

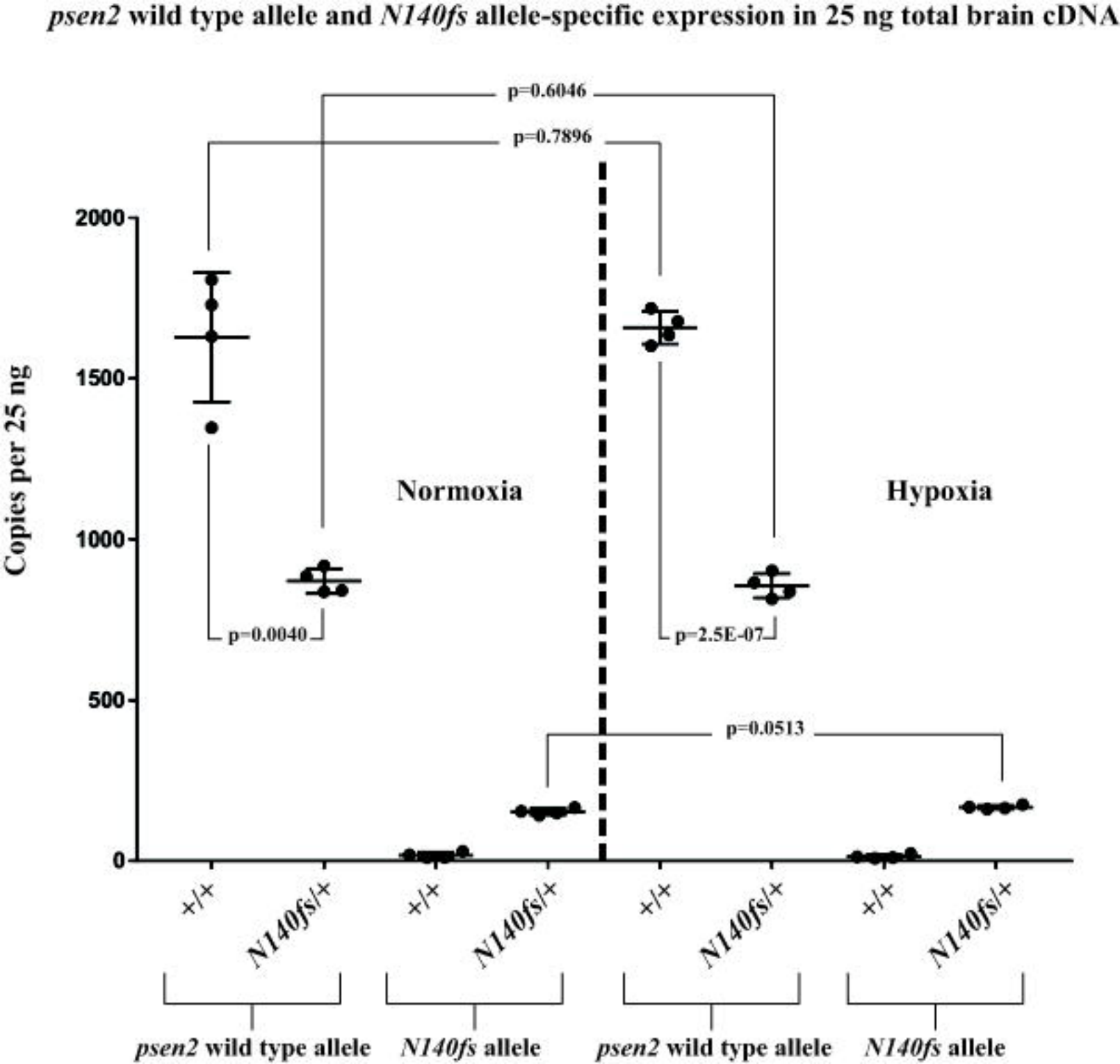
psen2 wild type allele and N140fs allele-specific expression in 25 ng total brain cDNA
p=0.6046
p=0.7896
2000
1500
1000
500
0
Copies per 25 ng
Normoxia
Hypoxia
p=0.0040
p=2.5E-07
p=0.0513
+/+
N140fs/+
+/+
N140fs/+
+/+
N140fs/+
+/+
N140fs/+
psen2 wild type allele
N140fs allele
psen2 wild type allele
N140fs allele

A G0 fish

"N140I oligo" -injected

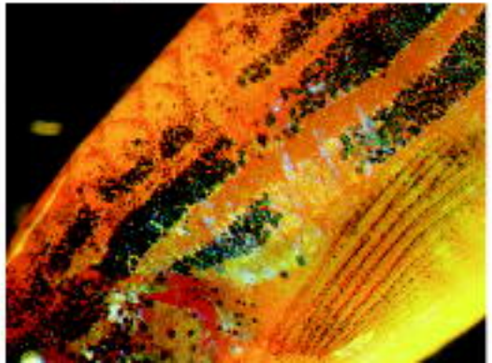

"V147I oligo" -injected

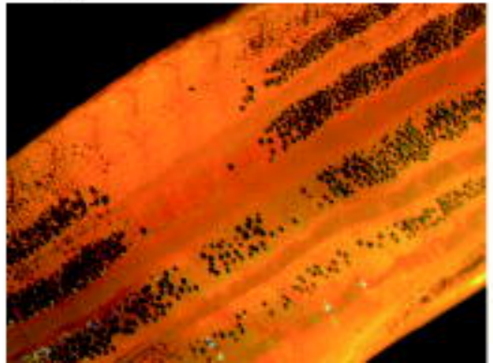

Uninjected

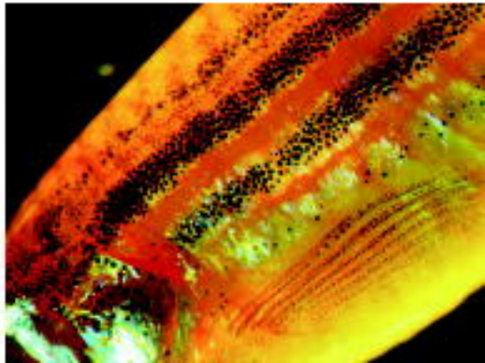

B T141_L142delinsMISLISV

	Homozygous	Heterozygous	Wildtype
1 month old	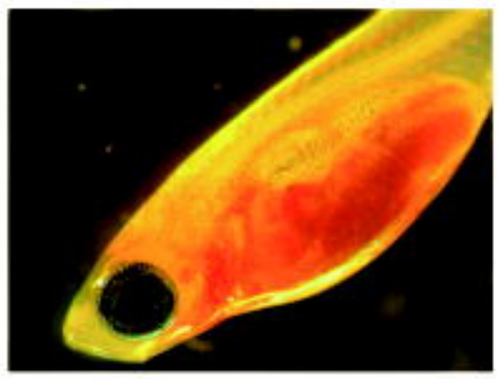	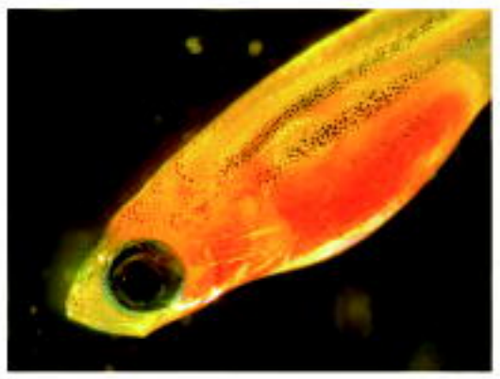	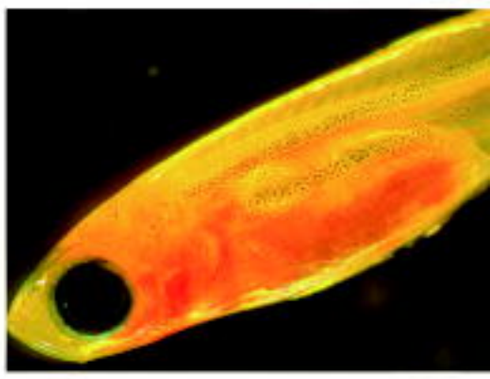
2 months old	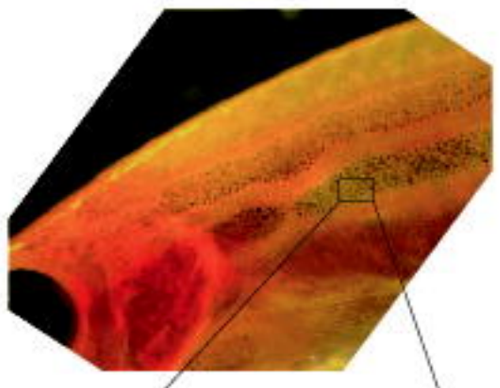 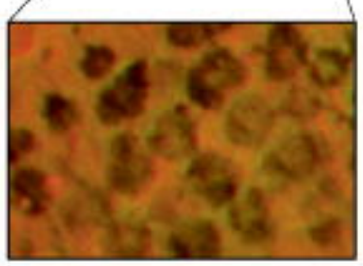	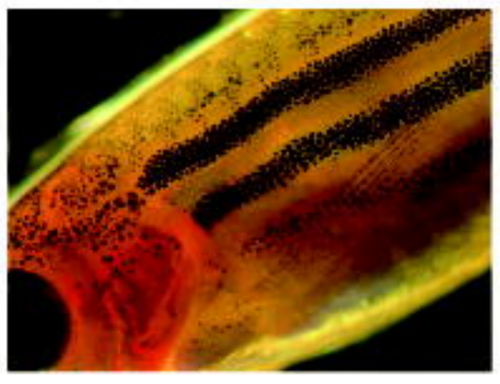	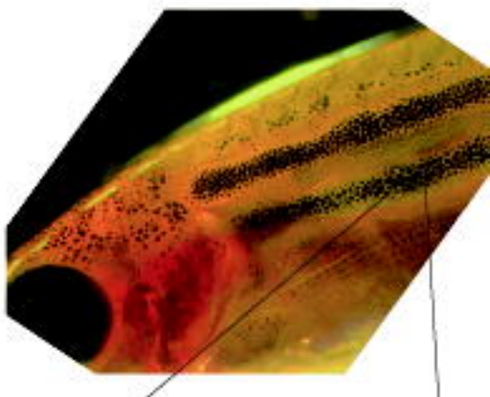 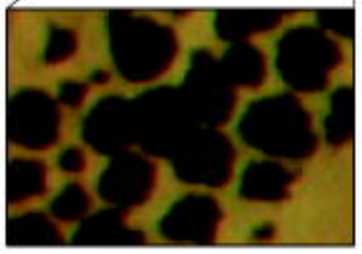
6 months old	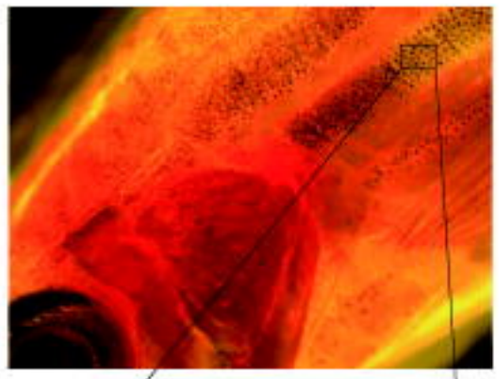 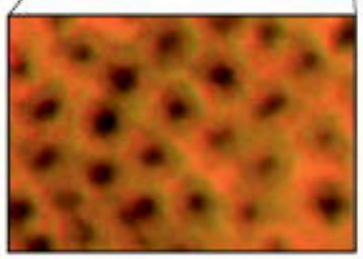	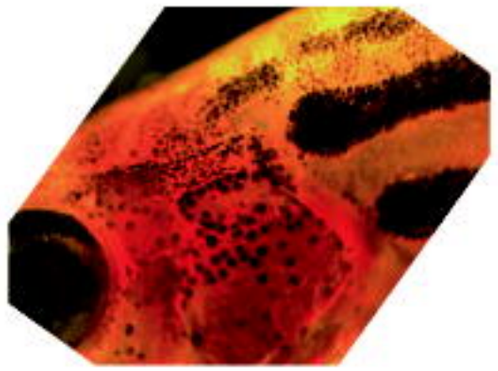	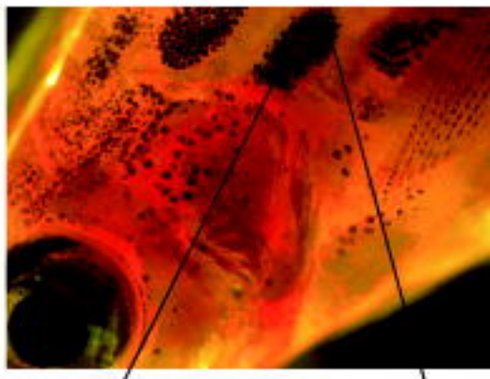 

C N140fs

	Homozygous	Heterozygous	Wildtype
1 month old	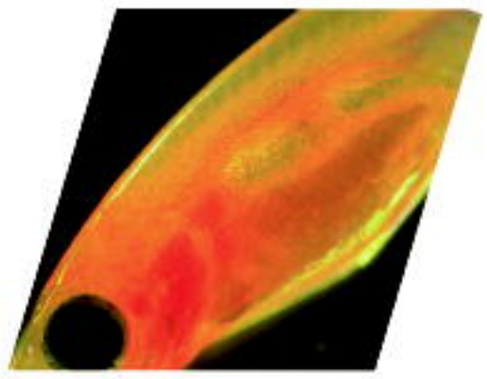	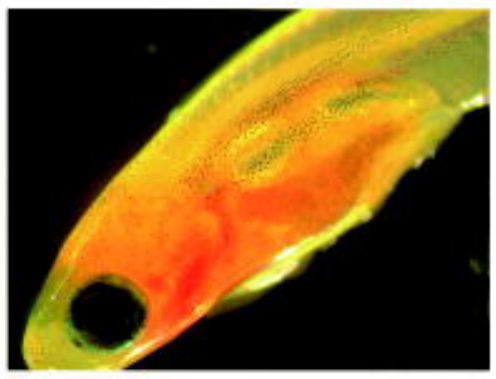	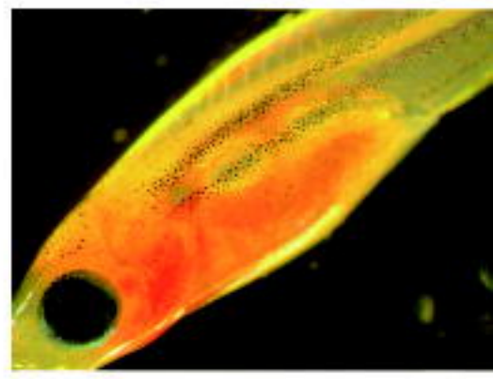
2 months old	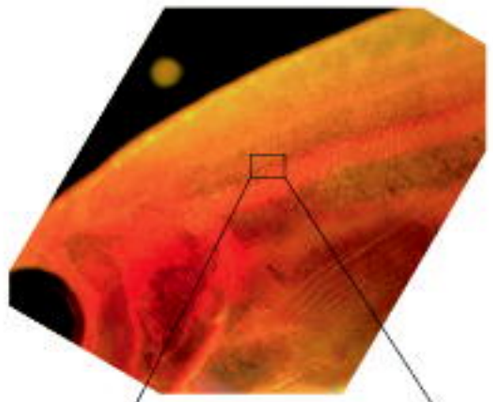 	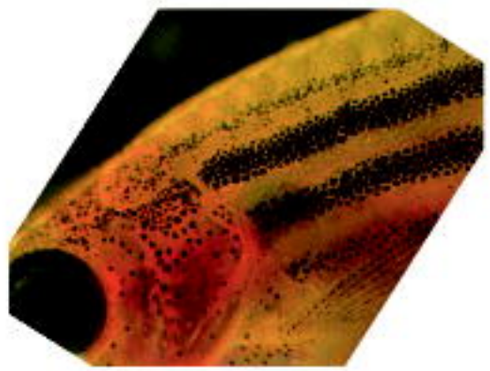	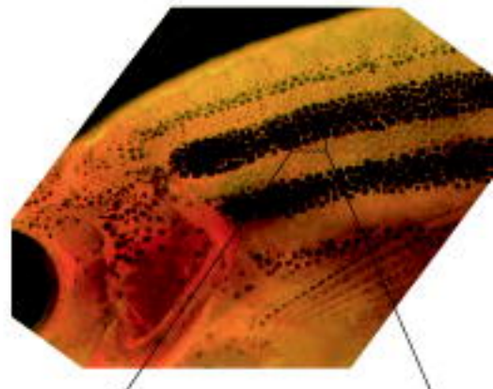 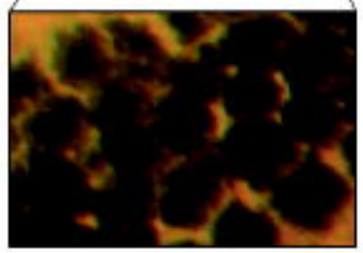
6 months old	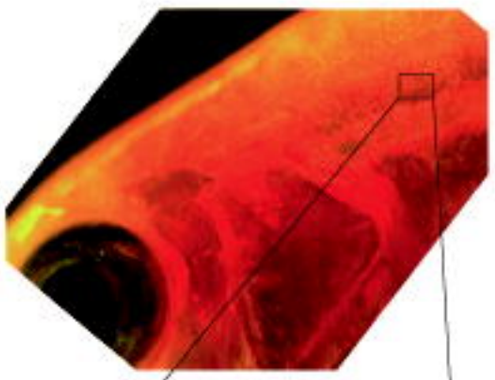 	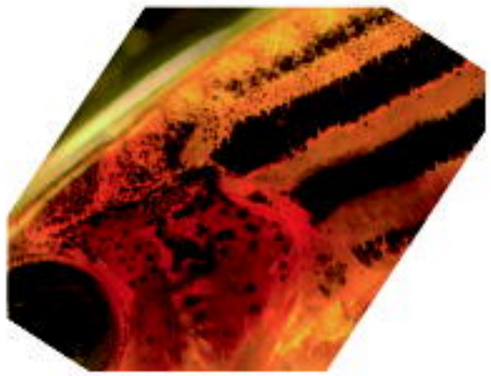	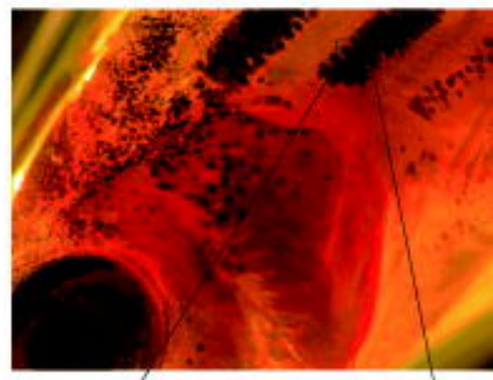 

D

48 hpf

+/+

N140fs/N140fs

A

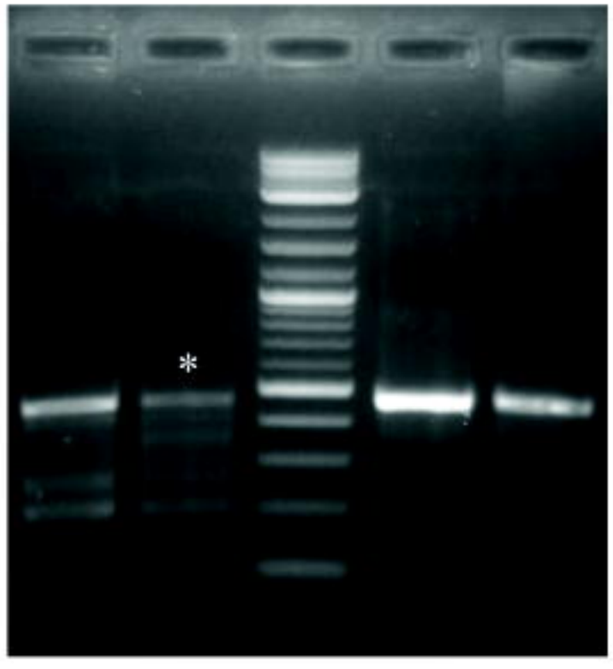

Lane

With T7 endonuclease I
1. - Uninjected TU embryos
2. - Target-sgRNA + Cas9 protein injected TU embryos

3. - 2 Log DNA size marker

Without T7 endonuclease I
4. - Uninjected TU embryos
5. - Target-sgRNA + Cas9 protein injected TU embryos

B

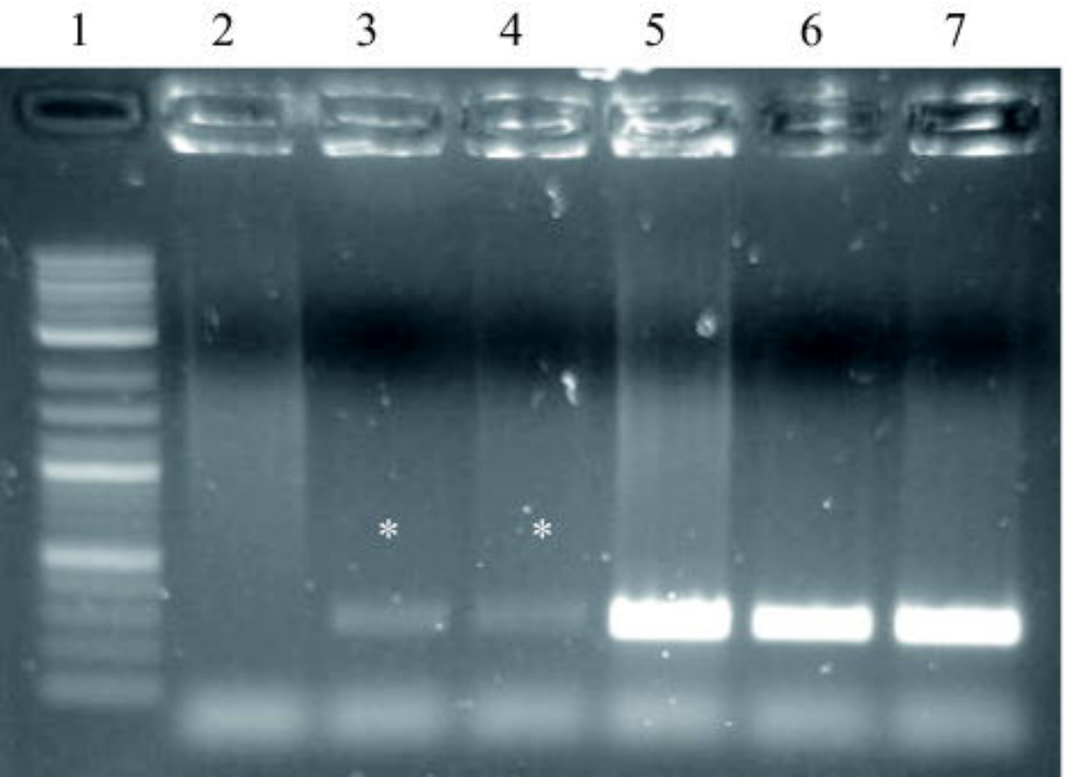

Lane

1. - 2 Log DNA size marker

"N140I" allele-specific detection PCR
2. - Uninjected TU embryos
3. - "N140I oligo" + CRISPR/Cas9 system injected TU embryos 1st batch
4. - "N140I oligo" + CRISPR/Cas9 system injected TU embryos 2nd batch

Wild type allele-specific detection PCR
5. - Uninjected TU embryos
6. - "N140I oligo" + CRISPR/Cas9 system injected TU embryos 1st batch
7. - "N140I oligo" + CRISPR/Cas9 system injected TU embryos 2nd batch

C

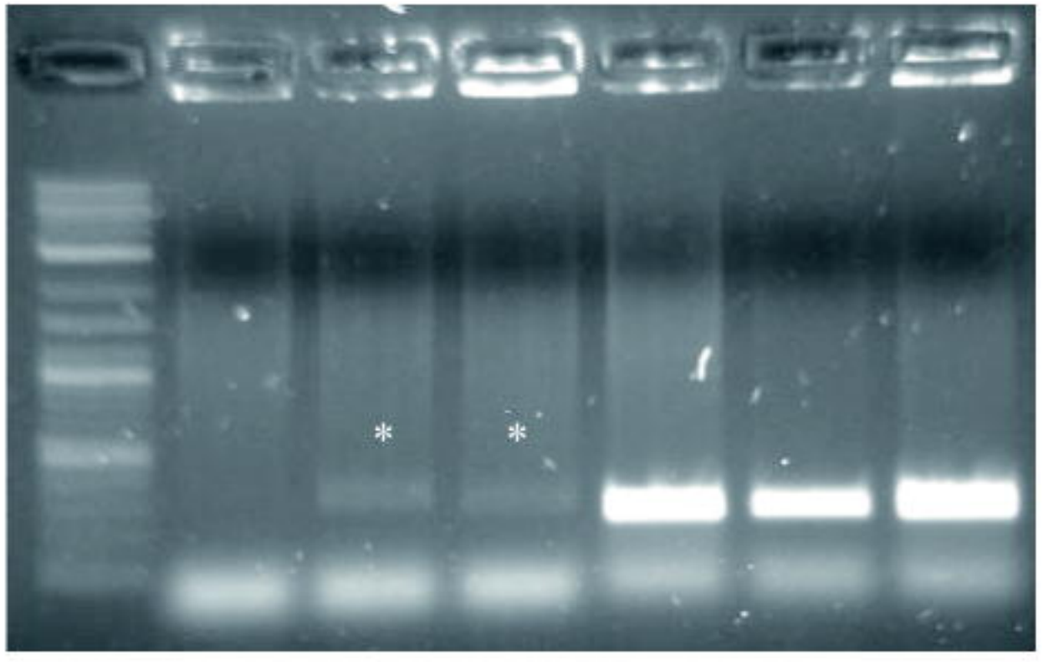

1. - 2 Log DNA size marker

"V147I" allele-specific detection PCR
2. - Uninjected TU embryos
3. - "V147I oligo" + CRISPR/Cas9 system injected TU embryos 1st batch
4. - "V147I oligo" + CRISPR/Cas9 system injected TU embryos 2nd batch

Wild type allele-specific detection PCR
5. - Uninjected TU embryos
6. - "V147I oligo" + CRISPR/Cas9 system injected TU embryos 1st batch
7. - "V147I oligo" + CRISPR/Cas9 system injected TU embryos 2nd batch

D

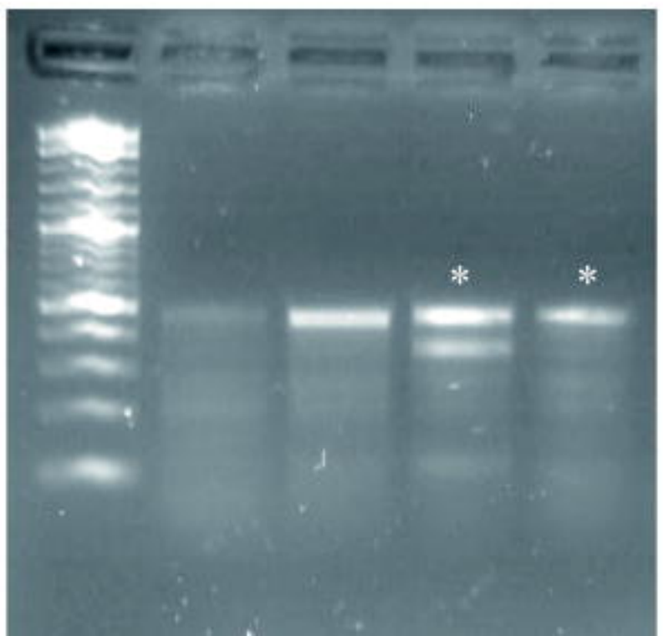

Lane

With T7 endonuclease I
1. - 2 Log DNA size marker
2. - Uninjected TU embryos
3. - F1 fish without any random mutation (wildtype)
4. - F1 fish with a random mutation (heterozygous mutant)
5. - F1 fish with a random mutation (heterozygous mutant)

A

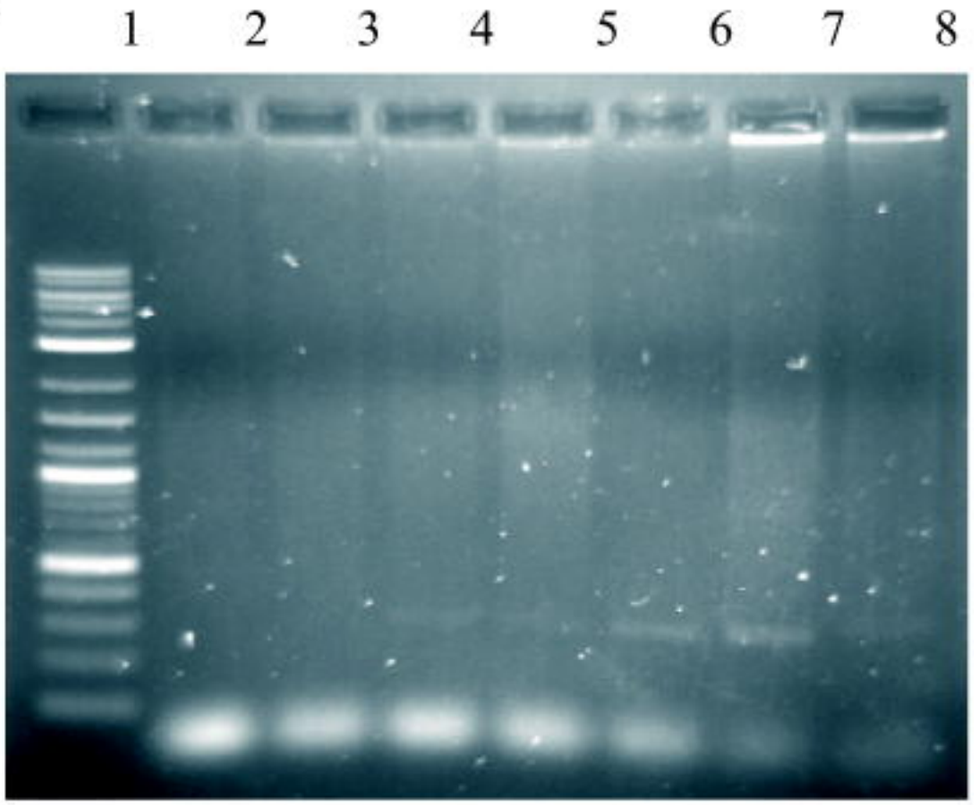

Lane

1. - 2 Log DNA size marker

“N140I” allele-specific detection PCR
2. - Uninjected TU embryos
3. - “N140I”-positive Fish F0_1
4. - “N140I”-positive Fish F0_2
5. - “N140I”-positive Fish F0_3
6. - “N140I”-positive Fish F0_4
7. - “N140I”-positive Fish F0_5
8. - “N140I”-positive Fish F0_6

B

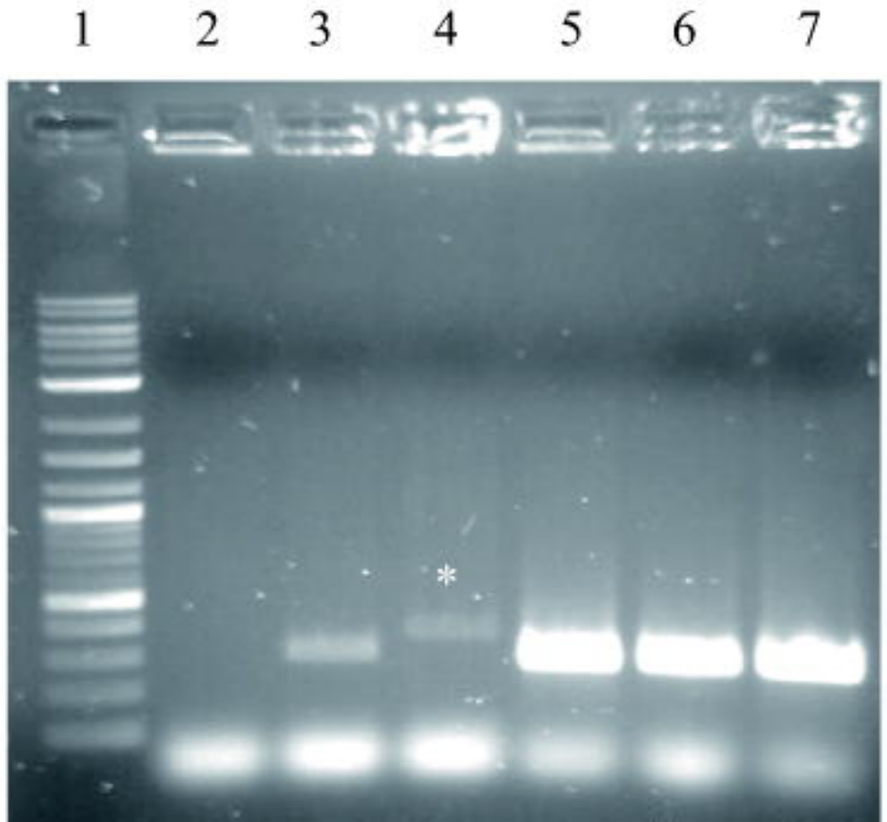

Lane

1. - 2 Log DNA size marker

“N140I” allele-specific detection PCR
2. - Uninjected TU embryos
3. - “N140I oligo” + CRISPR/Cas9 system injected TU embryos 2nd batch
4. - embryos from “N140I”-positive Fish F0_12 crossing TU wildtype fish

Wild type allele-specific detection PCR
5. - Uninjected TU embryos
6. - “N140I oligo” + CRISPR/Cas9 system injected TU embryos 2nd batch
7. - embryos from “N140I”-positive Fish F0_12 crossing TU wildtype fish

C

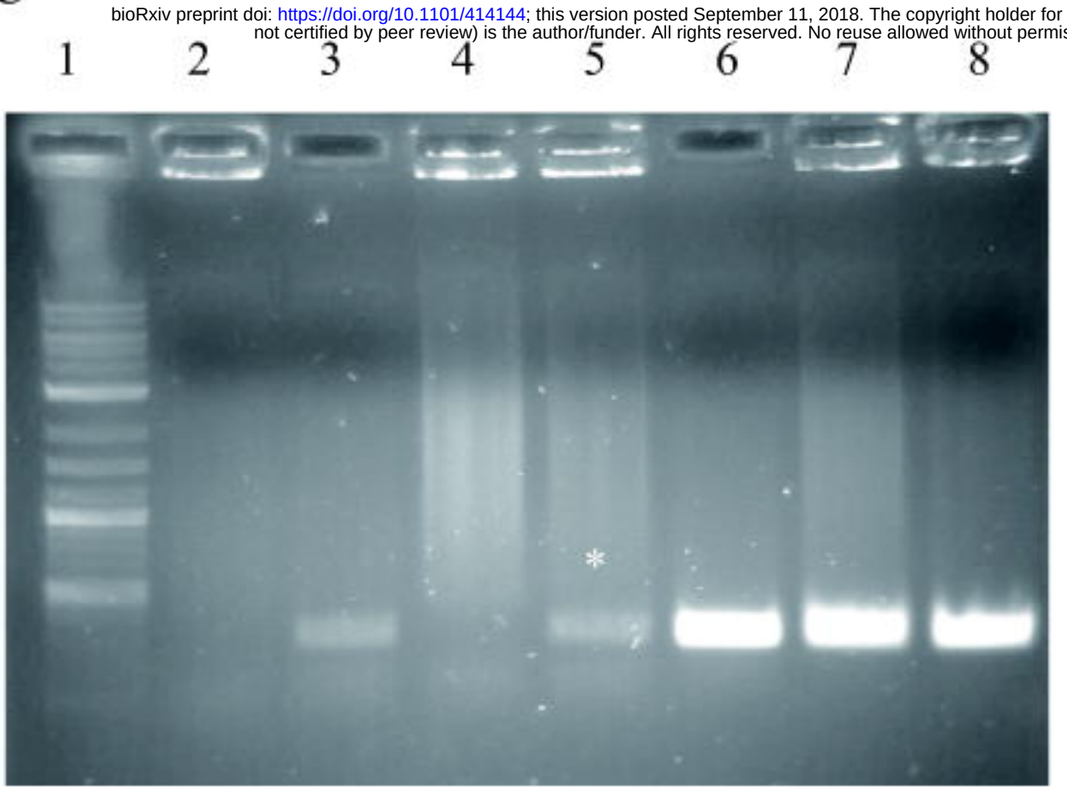

Lane

1. - 2 Log DNA size marker

“V147I” allele-specific detection PCR
2. - Uninjected TU embryos
3. - “V147I oligo” + CRISPR/Cas9 system injected TU embryos 1nd batch
4. - embryos from “V147I”-positive Fish F0_1 crossing TU wildtype fish
5. - embryos from “V147I”-positive Fish F0_3 crossing TU wildtype fish

Wild type allele-specific detection PCR
6. - “V147I oligo” + CRISPR/Cas9 system injected TU embryos 1nd batch
7. - embryos from “V147I”-positive Fish F0_1 crossing TU wildtype fish
8. - embryos from “V147I”-positive Fish F0_3 crossing TU wildtype fish

D

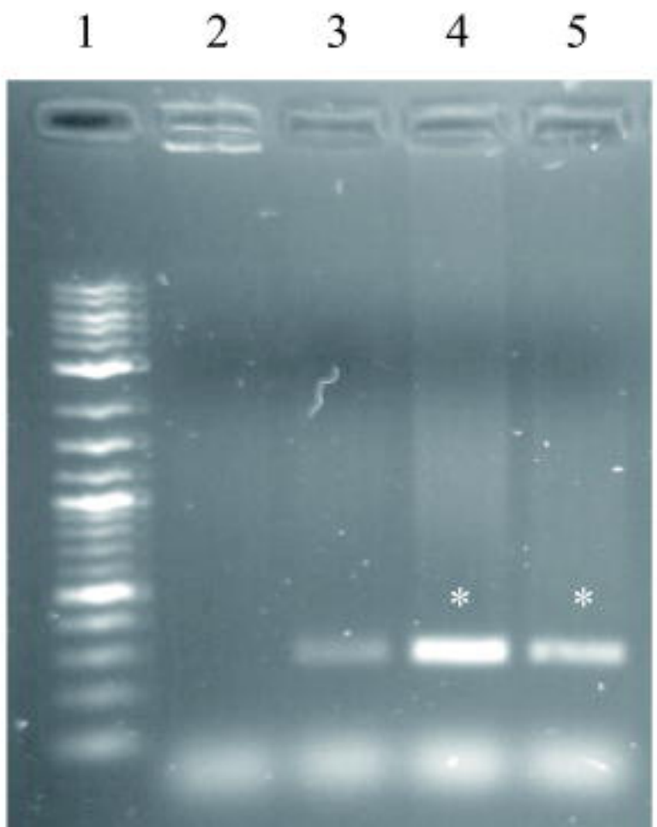

Lane

1. - 2 Log DNA size marker

“V147I” allele-specific detection PCR
2. - Uninjected TU embryos
3. - embryos from “V147I”-positive Fish F0_3 crossing TU wildtype fish
4. - Fish F1_2 form “V147I”-positive Fish F0_3 crossing TU wildtype fish
5. - Fish F1_8 form “V147I”-positive Fish F0_3 crossing TU wildtype fish

E

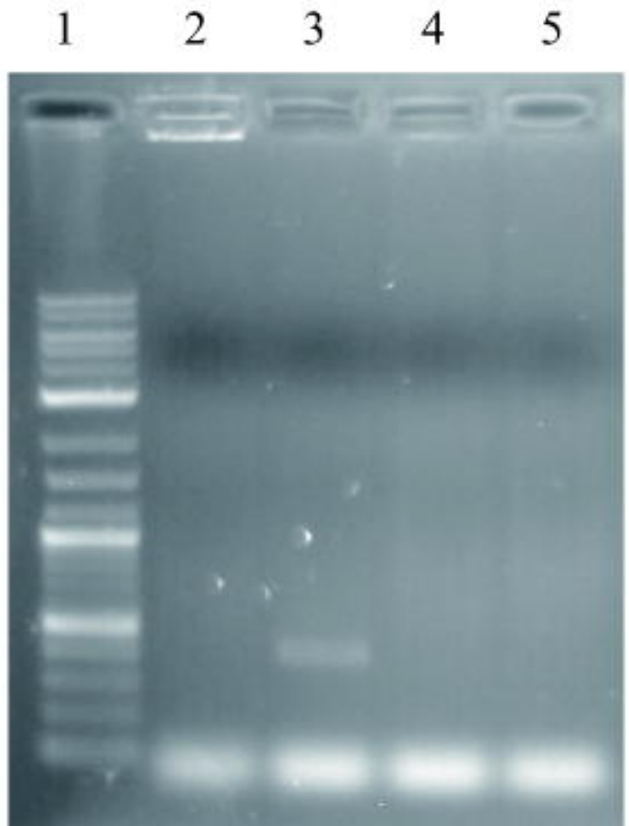

Lane

1. - 2 Log DNA size marker

"V147I" allele-specific detection PCR (with the reverse primer of T7 endonuclease I assay)
2. - Uninjected TU embryos
3. - embryos from "V147I"-positive Fish F0_3 crossing TU wildtype fish
4. - Fish F1_2 form "V147I"-positive Fish F0_3 crossing TU wildtype fish
5. - Fish F1_8 form "V147I"-positive Fish F0_3 crossing TU wildtype fish

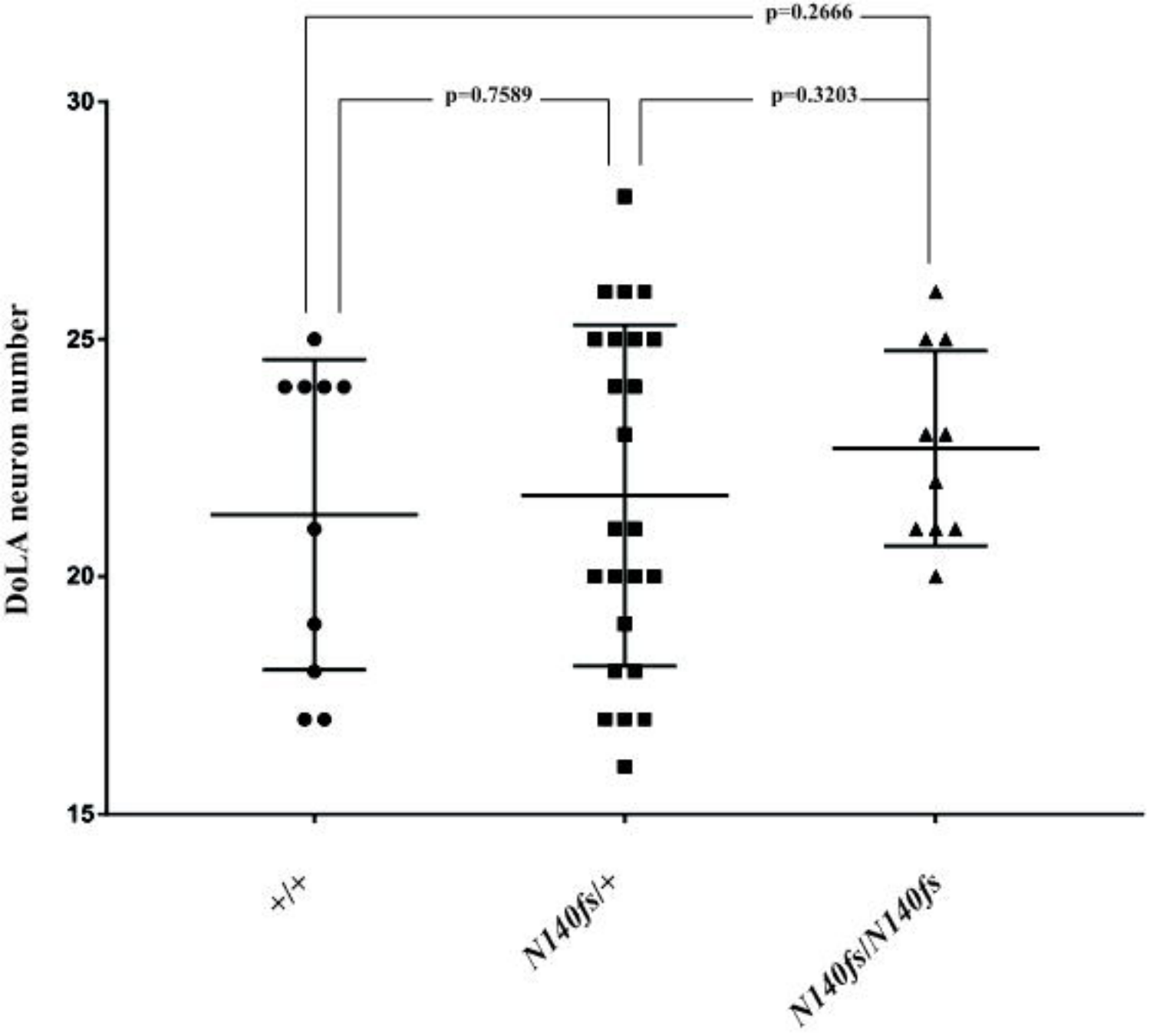
p=0.2666
p=0.7589
p=0.3203
30
25
20
15
DoLA neuron number
+/+
N140fs/+
N140fs/N140fs

A

Lane

1. - Non-treated *N140fs*/+ embryos
2. - CHX-treated *N140fs*/+ embryos

B